Cohen, S.E., Kokkotou, E., Biddinger, S.B., Kondo, T., Gebhardt, R., Kratzsch, J., Mantzoros, C.S., and Kahn, C.R. (2007). High circulating leptin receptors with normal leptin sensitivity in liver-specific insulin receptor knock-out (LIRKO) mice. J. Biol. Chem. *282*, 23672–23678.

Dong, X., Park, S., Lin, X., Copps, K., Yi, X., and White, M.F. (2006). Irs1 and Irs2 signaling is essential for hepatic glucose homeostasis and systemic growth. J. Clin. Invest. *116*, 101–114.

Gribble, F.M. (2005). Metabolism: a higher power for insulin. Nature *434*, 965–966.

Hirashima, Y., Tsuruzoe, K., Kodama, S., Igata, M., Toyonaga, T., Ueki, K., Kahn, C.R., and Araki, E. (2003). Insulin down-regulates insulin receptor substrate-2 expression through the phosphatidylinositol 3-kinase/Akt pathway. J. Endocrinol. *179*, 253–266.

Kasuga, M. (2006). Insulin resistance and pancreatic beta cell failure. J. Clin. Invest. *116*, 1756–1760.

Kops, G.J., de Ruiter, N.D., de Vries-Smits, A.M., Powell, D.R., Bos, J.L., and Burgering, B.M. (1999). Direct control of the Forkhead transcription factor AFX by protein kinase B. Nature *398*, 630–634.

Kubota, N., Terauchi, Y., Miki, H., Tamemoto, H., Yamauchi, T., Komeda, K., Satoh, S., Nakano, R., Ishii, C., Sugiyama, T., et al. (1999). PPAR gamma mediates high-fat diet-induced adipocyte hypertrophy and insulin resistance. Mol. Cell *4*, 597–609.

Kubota, N., Tobe, K., Terauchi, Y., Eto, K., Yamauchi, T., Suzuki, R., Tsubamoto, Y., Komeda, K., Nakano, R., Miki, H., et al. (2000). Disruption of insulin receptor substrate 2 causes type 2 diabetes because of liver insulin resistance and lack of compensatory beta-cell hyperplasia. Diabetes *49*, 1880–1889.

Kubota, N., Terauchi, Y., Tobe, K., Yano, W., Suzuki, R., Ueki, K., Takamoto, I., Satoh, H., Maki, T., Kubota, T., et al. (2004). Insulin receptor substrate 2 plays a crucial role in beta cells and the hypothalamus. J. Clin. Invest. *114*, 917–927.

Kubota, N., Terauchi, Y., Kubota, T., Kumagai, H., Itoh, S., Satoh, H., Yano, W., Ogata, H., Tokuyama, K., Takamoto, I., et al. (2006). Pioglitazone ameliorates insulin resistance and diabetes by both adiponectin-dependent and -independent pathways. J. Biol. Chem. *281*, 8748–8755.

Lo, S., Russell, J.C., and Taylor, A.W. (1970). Determination of glycogen in small tissue samples. J. Appl. Physiol. *28*, 234–236.

Matsumoto, M., Ogawa, W., Teshigawara, K., Inoue, H., Miyake, K., Sakaue, H., and Kasuga, M. (2002). Role of the insulin receptor substrate 1 and phosphatidylinositol 3-kinase signaling pathway in insulin-induced expression of sterol regulatory element binding protein 1c and glucokinase genes in rat hepatocytes. Diabetes *51*, 1672–1680.

Michael, M.D., Kulkarni, R.N., Postic, C., Previs, S.F., Shulman, G.I., Magnuson, M.A., and Kahn, C.R. (2000). Loss of insulin signaling in hepatocytes leads to severe insulin resistance and progressive hepatic dysfunction. Mol. Cell *6*, 87–97.

Nakae, J., Park, B.C., and Accili, D. (1999). Insulin stimulates phosphorylation of the forkhead transcription factor FKHR on serine 253 through a Wortmannin-sensitive pathway. J. Biol. Chem. *274*, 15982–15985.

Nakae, J., Kitamura, T., Silver, D.L., and Accili, D. (2001). The forkhead transcription factor FoxO1 (Fkhr) confers insulin sensitivity onto glucose-6-phosphatase expression. J. Clin. Invest. *108*, 1359–1367.

Nandi, A., Kitamura, Y., Kahn, C.R., and Accili, D. (2004). Mouse models of insulin resistance. Physiol. Rev. *84*, 623–647.

Obici, S., Feng, Z., Karkanias, G., Baskin, D.G., and Rossetti, L. (2002a). Decreasing hypothalamic insulin receptors causes hyperphagia and insulin resistance in rats. Nat. Neurosci. *5*, 566–572.

Obici, S., Zhang, B.B., Karkanias, G., and Rossetti, L. (2002b). Hypothalamic insulin signaling is required for inhibition of glucose production. Nat. Med. *8*, 1376–1382.

Plum, L., Belgardt, B.F., and Bruning, J.C. (2006). Central insulin action in energy and glucose homeostasis. J. Clin. Invest. *116*, 1761–1766.

Previs, S.F., Withers, D.J., Ren, J.M., White, M.F., and Shulman, G.I. (2000). Contrasting effects of Irs-1 versus Irs-2 gene disruption on carbohydrate and lipid metabolism in vivo. J. Biol. Chem. *275*, 38990–38994.

Saltiel, A.R., and Kahn, C.R. (2001). Insulin signalling and the regulation of glucose and lipid metabolism. Nature *414*, 799–806.

Simmgen, M., Knauf, C., Lopez, M., Choudhury, A.I., Charalambous, M., Cantley, J., Bedford, D.C., Claret, M., Iglesias, M.A., Heffron, H., et al. (2006). Liver-specific deletion of insulin receptor substrate 2 does not impair hepatic glucose and lipid metabolism in mice. Diabetologia *49*, 552–561.

Tamemoto, H., Kadowaki, T., Tobe, K., Yagi, T., Sakura, H., Hayakawa, T., Terauchi, Y., Ueki, K., Kaburagi, Y., Satoh, S., et al. (1994). Insulin resistance and growth retardation in mice lacking insulin receptor substrate-1. Nature *372*, 182–186.

Taniguchi, C.M., Ueki, K., and Kahn, R. (2005). Complementary roles of Irs-1 and Irs-2 in the hepatic regulation of metabolism. J. Clin. Invest. *115*, 718–727.

Taniguchi, C.M., Emanuelli, B., and Kahn, C.R. (2006). Critical nodes in signalling pathways: insights into insulin action. Nat. Rev. Mol. Cell Biol. *7*, 85–96.

Thirone, A.C., Huang, C., and Klip, A. (2006). Tissue-specific roles of IRS proteins in insulin signaling and glucose transport. Trends Endocrinol. Metab. *17*, 72–78.

Tobe, K., Tamemoto, H., Yamauchi, T., Aizawa, S., Yazaki, Y., and Kadowaki, T. (1995). Identification of a 190-kDa protein as a novel substrate for the insulin receptor kinase functionally similar to insulin receptor substrate-1. J. Biol. Chem. *270*, 5698–5701.

Tobe, K., Suzuki, R., Aoyama, M., Yamauchi, T., Kamon, J., Kubota, N., Terauchi, Y., Matsui, J., Akanuma, Y., Kimura, S., et al. (2001). Increased expression of the sterol regulatory element-binding protein-1 gene in insulin receptor substrate-2(−/−) mouse liver. J. Biol. Chem. *276*, 38337–38340.

Wada, A., Yokoo, H., Yanagita, T., and Kobayashi, H. (2005). New twist on neuronal insulin receptor signaling in health, disease, and therapeutics. J. Pharmacol. Sci. *99*, 128–143.

Withers, D.J., Gutierrez, J.S., Towery, H., Burks, D.J., Ren, J.M., Previs, S., Zhang, Y., Bernal, D., Pons, S., Shulman, G.I., et al. (1998). Disruption of Irs-2 causes type 2 diabetes in mice. Nature *391*, 900–904.

Yamauchi, T., Tobe, K., Tamemoto, H., Ueki, K., Kaburagi, Y., Yamamoto-Honda, R., Takahashi, Y., Yoshizawa, F., Aizawa, S., Akanuma, Y., et al. (1996). Insulin signalling and insulin actions in the muscles and livers of insulin-resistant, insulin receptor substrate 1-deficient mice. Mol. Cell. Biol. *16*, 3074–3084.

Yamauchi, T., Kamon, J., Ito, Y., Tsuchida, A., Yokomizo, T., Kita, S., Sugiyama, T., Miyagishi, M., Hara, K., Tsunoda, M., et al. (2003). Cloning of adiponectin receptors that mediate antidiabetic metabolic effects. Nature *423*, 762–769.

Zhang, J., Ou, J., Bashmakov, Y., Horton, J.D., Brown, M.S., and Goldstein, J.L. (2001). Insulin inhibits transcription of IRS-2 gene in rat liver through an insulin response element (IRE) that resembles IREs of other insulin-repressed genes. Proc. Natl. Acad. Sci. USA *98*, 3756–3761.

Clin Exp Med (2008) 8:93–99
DOI 10.1007/s10238-008-0163-1

ORIGINAL

Fulminant type 1 diabetes mellitus observed in insulin receptor substrate 2 deficient mice

T. Arai · H. Hashimoto · K. Kawai · A. Mori · Y. Ohnishi · K. Hioki · M. Ito · M. Saito · Y. Ueyama · M. Ohsugi · R. Suzuki · N. Kubota · T. Yamauchi · K. Tobe · T. Kadowaki · K. Kosaka

Received: 14 October 2007 / Accepted: 20 December 2007

Abstract The objective of this study was to characterise the fulminant type 1 diabetes mellitus (DM) accompanying abrupt hyperglycaemia and ketonuria observed in insulin receptor substrate 2 (IRS2)-deficient mice. IRS2-deficient mice backcrossed onto the original C57BL/6J:Jcl background (B6J-IRS2$^{-/-}$ mice) for more than 10 generations were used. Eight male IRS2-deficient mice with ketonuria and abrupt increase in plasma glucose concentrations over 25 mmol/l were used as the fulminant type 1 diabetic mice (diabetic mice) and 8 male IRS2-deficient mice (8 weeks old) without glycosuria were used as the control mice. Plasma metabolite, immunoreactive insulin (IRI) and C-peptide concentrations, hepatic energy metabolism related enzyme activities and histopathological change in pancreatic islets were investigated. The diabetic mice showed significantly higher plasma glucose and cholesterol concentrations and lower plasma IRI and C-peptide concentrations than the control mice. In livers of the diabetic mice, glycolytic and malate-aspartate shuttle enzyme activities decreased significantly and gluconeogenic, lipogenic and ketone body synthesis enzyme activities increased significantly compared to those in the control mice. The pancreatic islets of the diabetic mice decreased significantly in size and number of β cells. The diabetic IRS2-deficient mice did not show the islet-related antibodies observed in the diabetic NOD mice in their sera. The characteristics of the diabetic IRS2-deficient mice resembled those of the human nonautoimmune fulminant type 1 DM. IRS2-deficient mice may be a useful animal model for studying the degradation mechanism of pancreatic β cells in the process of development of fulminant type 1 DM.

Keywords Insulin · IRS2 knockout mouse · Ketone body · Liver · Type 1 diabetes mellitus

T. Arai (✉)
Department of Veterinary Science,
School of Veterinary Medicine,
Nippon Veterinary and Life Science University,
1-7-1 Kyonancho, Musashino, Tokyo 180-8602, Japan
e-mail: tarai@nvlu.ac.jp

H. Hashimoto · K. Kawai · Y. Ohnishi · K. Hioki · M. Ito · M. Saito
Animal Resource Center,
Central Institute for Experimental Animals,
Kawasaki, Japan

A. Mori
Department of Veterinary Science,
School of Veterinary Medicine,
Nippon Veterinary and Life Science University,
Musashino, Japan

Y. Ueyama
Department of Pathology,
Tokai University School of Medicine,
Isehara, Japan

M. Ohsugi · R. Suzuki · N. Kubota · T. Yamauchi · K. Tobe · T. Kadowaki · K. Kosaka
Department of Metabolic Diseases,
Graduate School of Medicine,
University of Tokyo, Tokyo, Japan

Introduction

Insulin receptor substrate (IRS) disorders are associated with onset of insulin resistance, obesity and diabetes mellitus (DM) [1–3]. IRS1-deficient mice are growth-retarded

and show skeletal muscle insulin resistance [1] but do not develop DM because the hyperinsulinaemia associated with the β-cell hyperplasia in these mice effectively compensates for the insulin resistance [4, 5]. IRS2-deficient ($IRS2^{-/-}$) mice develop DM, presumably due to inadequate β-cell proliferation combined with insulin resistance [6, 7], and the insulin resistance in IRS2-deficient mice is ameliorated by reduction of adiposity [3]. IRS2-deficient mice are widely used for analysis of pathophysiology of human type 2 DM. In IRS2-deficient mice (C57BL/6×CBA hybrid background) generated by Kubota and others [8] with C57BL/6J:Jcl mice to establish an inbred line of IRS2-deficient mice, serious type 1 diabetes accompanied by abrupt and marked increase of their plasma glucose concentrations and ketonuria was sometimes observed [9]. The symptoms observed in IRS2-deficient mice with serious type 1 DM with insulin-deficient hyperglycaemia resembled those of the human nonautoimmune fulminant type 1 DM reported by Imagawa and others [10–12]. In the present study, concentrations of plasma metabolite, insulin and C-peptide, activities of hepatic enzymes related to energy metabolism, and histopathological changes in pancreas and islet-related antibodies were investigated to characterise serious DM with abrupt onset of insulin-deficient hyperglycaemia observed in IRS2 deficiency and to evaluate the usefulness of IRS2-deficient mice as an animal model for studying fulminant type 1 DM of humans.

Materials and methods

Mice

IRS2-deficient mice were backcrossed onto the original C57BL/6J:Jcl background (B6J-$IRS2^{-/-}$ mice) for more than 10 generations. B6J-$IRS2^{-/-}$ and wild-type mice were prepared by intercrossing with B6J-$IRS2^{-/+}$ mice, which were used for *in vitro* fertilisation and embryo transfer. All mice were provided with a premium feed for laboratory animals (CA-1, CLEA, Tokyo, Japan) and tap water *ad libitum*. After weaning, 2–3 mice were housed together in each open cage. The animal room was maintained at 24 ± 2°C and at 55 ± 10% relative humidity on a 12:12-h light:dark cycle (light on 8:00 to 20:00). Concentrations of blood glucose taken from the orbital sinus of mice using a heparinised capillary tube were monitored weekly using an automatic blood glucose meter (Arkray, Kyoto, Japan). Eight male IRS2-deficient mice (8 weeks old) without glycosuria according to Diasticks (Bayer Medical Ltd., Tokyo, Japan) were used as the control, because over 50% of male IRS2-deficient mice after 10 weeks of age tended to show glycosuria with obesity. Eight IRS2-deficient mice (8–20 weeks old) with abrupt increase of blood glucose concentrations over 25mmol/l within a week and ketonuria with ketosticks (Bayer Medical Ltd., Tokyo, Japan) were determined as fulminant type 1 diabetic mice.

Sample preparation

Blood and liver were taken from mice anaesthetised with pentobarbital sodium (40 mg/kg, intraperitoneally) and euthanised between 11:00 and 14:00. Plasma was isolated by centrifugation at 4°C. Liver was excised, quick-frozen in liquid nitrogen, and stored at –80°C for subsequent analysis. Cytosolic and mitochondrial fractions were prepared from the frozen liver by the reported method [13].

Chemical analysis

Plasma glucose concentrations were measured by the glucose oxidase method [14] and immunoreactive insulin (IRI) concentrations were determined by the ELISA described previously [15]. Plasma C-peptide, free fatty acid (FFA), triglyceride (TG) and total cholesterol concentrations were determined using commercial kits purchased from Wako Pure Chemical Industries (Tokyo, Japan).

Enzyme activity assay

Activities of enzymes in hepatic cytosolic and mitochondrial fractions were measured by the previously reported methods: hexokinase (HK) and glucokinase (GK) [16], glucose 6-phosphate dehydrogenase (G6PD) [17], lactate dehydrogenase (LDH) [18], malate dehydrogenase (MDH) [19], aspartate aminotransferase (AST) [20], phosphoenolpyruvate carboxykinase (PEPCK) [21], fructose 1,6-bisphosphatase (FBPase) [22], ATP citrate lyase (ACL) [23], malic enzyme [24], fatty acid synthase (FAS) [25], glutamate dehydrogenase (GLDH) [26], 3-hydrobutyrate dehydrogenase (3HBD) [27] and pyruvate carboxylase (PC) [28]. Enzyme activity was measured at 25 ± 2°C and expressed as nanomoles of substrate degraded per minute per milligram of protein. Protein concentrations were determined by the method of Bradford [29] with bovine serum albumin (Wako Pure Chemical Industries) as the standard. Activities of HK and GK as rate-limiting enzymes in glycolysis, G6PD as rate-limiting enzyme in pentose-phosphate pathway, LDH as cytosol marker enzyme, MDH and AST as crucial enzymes in the malate-aspartate shuttle, PEPCK and FBPase as rate-limiting enzymes in gluconeogenesis, ACL, malic enzyme and FAS as rate-limiting enzymes in fatty acid synthesis, PC as oxaloacetate-supplying enzyme to the tricarboxylic acid (TCA) cycle, GLDH as mito-

chondrial marker enzyme and 3HBD as rate-limiting enzyme in ketone body synthesis were measured.

Immunohistochemistry of pancreatic islet cells

Removed pancreas of the control and the diabetic mice (12 weeks old, plasma glucose, 31.1 mmol/l; plasma IRI, 36 pmol/l) were placed in 10% buffered formalin, embedded in paraffin and sectioned at a thickness of 4 μm. Sections were pretreated with 0.03% H_2O_2 in methanol to block endogenous peroxidase activity, and incubated for 60 min at room temperature with guinea pig anti-swine insulin (DakoCytomation, Code No.: N1542), followed by 30 min incubation with peroxidase-conjugated rabbit anti-guinea pig immunoglobulins (Dako A/S, Code No: P0141). Then, the sections were incubated for 60 min at room temperature with rabbit anti-human glucagon (DakoCytomation), followed by 30 min incubation with alkaline phosphatase-labelled polymer conjugated goat anti-rabbit antibody (Nichirei, Code No.: 414251). For double staining, peroxidase (brown, DAB) and alkaline phosphatase (red, New Fuchsin) were used, respectively. The antigen-antibody reaction was visualised by incubation in 0.05 M Tris–HCl buffer (pH7.6) containing 0.02% 3,3'-diaminobenzidine and 0.006% H_2O_2 and New Fuchsin Substrate Kit (Nichirei, Code No.: 415161). Immunostained sections were counterstained with haematoxylin for visualisation of nuclei.

Observation of the islet-related antibodies in sera of mice

Existence of the islet-related antibodies was investigated immunohistochemically in sera of NOD mice as autoimmune type 1 diabetic model and IRS2-deficient mice using pancreatic sections prepared from mice before (control mice) and after (diabetic mice) onset of fulminant type 1 diabetes. All the pancreas specimens were fixed in 10% buffered formalin and embedded paraffin, mounted on amino-silane coated glass slides (Muto Pure Chemicals, Osaka, Japan) and stained using the indirect immunoperoxidase method. For each mouse, sera were treated with 0.03% H_2O_2 in methanol to measure the endogenous peroxidase activity. After pre-incubation with the 10% normal rabbit serum (Dako Cytomation, Glostrup, Denmark) for 10 min at room temperature, sections were then incubated with preclinical NOD/shi mice sera, diabetic NOD/shi mice sera, control IRS2 mice sera and diabetic IRS2 mice sera, followed by incubation overnight at 4°C. Sections were serially incubated with polyclonal rabbit anti-mouse immunoglobulins/HRP antibodies (Dako Cytomation, Glostrup, Denmark) for 60 min at room temperature. The peroxidase activity was visualised by incubation in a 0.05 M Tris-HCl buffer (pH7.6) containing 0.02% 3,3'-diaminobenzidine (DAB) and 0.006% H_2O_2 solution for 5 min. Immunostained sections were counterstained with haematoxylin for visualisation of nuclei.

Statistical analysis

All values are presented as means ± SE and differences between means were analysed by Student's *t*-test (Sigma Stat 3.0 for Windows, Hulinks, Tokyo, Japan). A p value less than 0.05 was considered statistically significant.

Results

The body weights of the diabetic mice were 26.0 ± 4.6 g (mean ± SD), smaller than those of the control mice (29.6 ± 3.8 g). As the diabetic mice (8–24 weeks of age) were older than the control mice (8 weeks of age), the reduction of body weights in the diabetic mice was significant. All the diabetic mice showed ketonuria. In the diabetic mice, the plasma glucose and cholesterol concentrations were significantly higher than those in the controls, whereas plasma IRI and C-peptide concentrations decreased significantly under one third of the control values. There were no significant differences in FFA and TG concentrations between the diabetic and control mice (Table 1). Activities of HK and GK in glycolysis and MDH in the malate-aspartate shuttle in the cytosolic fraction of liver in the diabetic mice were significantly

Table 1 Plasma metabolites, IRI and C-peptide concentrations in control and diabetic mice

	Control (8)	Diabetic (8)
Glucose (mmol/l)	12.4 ± 1.1	31.6 ± 4.3*
FFA (mEq/l)	1.0 ± 0.2	1.2 ± 0.3
TG (mmol/l)	0.9 ± 0.1	1.1 ± 0.2
Cholesterol (mmol/l)	2.3 ± 0.2	4.2 ± 0.7*
IRI (pmol/l)	240 ± 30	54 ± 12*
C-peptide (ng/ml)	3.4 ± 0.4	1.1 ± 0.3*

Values are presented as means ± SE
Numbers in parentheses indicate the number of animals examined
*$p < 0.05$ *vs.* controls

Table 2 Hepatic enzyme activities in control and diabetic mice

	Control (8)	Diabetic (8)
Cytosol HK	6.9 ± 0.5	4.7 ± 0.4*
GK	4.2 ± 0.6	1.3 ± 0.3*
G6PD	5.1 ± 0.5	4.6 ± 0.3
LDH	1294 ± 86	1108 ± 163
MDH	4288 ± 160	3499 ± 250*
AST	653 ± 75	615 ± 40
PEPCK	26 ± 3	31 ± 3
FBPase	68 ± 8	101 ± 6*
ACL	3.5 ± 0.4	3.5 ± 0.3
Malic enzyme	17 ± 2	30 ± 2*
FAS	4.7 ± 0.5	4.9 ± 0.8
Mitochondria GLDH	1834 ± 116	1635 ± 124
MDH	2480 ± 101	2524 ± 334
AST	1684 ± 62	1354 ± 52*
3-HBD	4.1 ± 0.2	8.6 ± 1.4*
PC	153 ± 8	66 ± 6*

Mean ± SE enzyme activities are presented as nmol of substrate degraded per min per mg protein
Numbers in parentheses indicate the number of animals examined
*$p < 0.05$ *vs.* controls

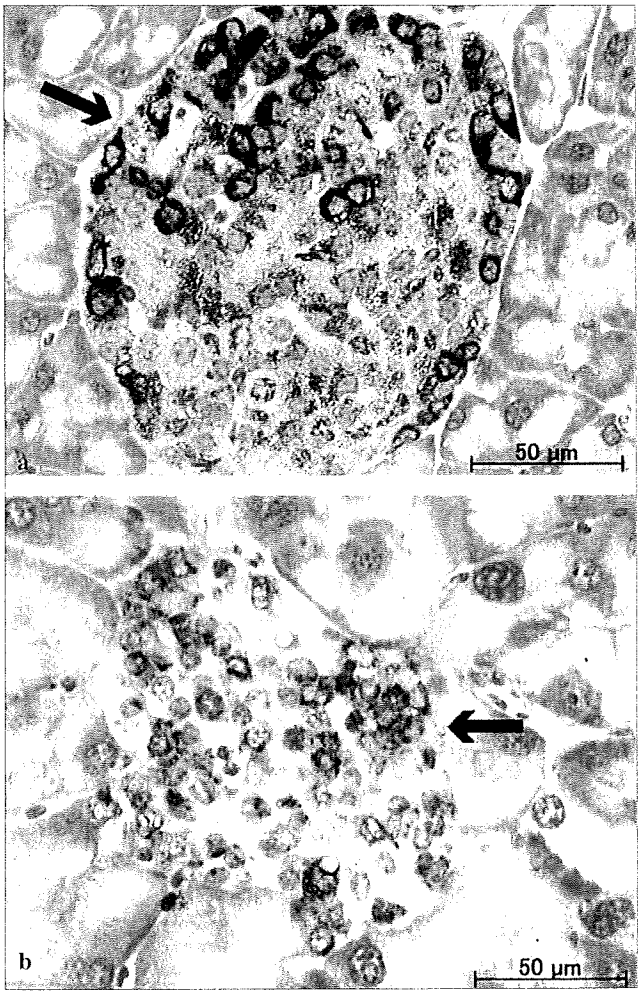

Fig. 1 Histopathological examinations of pancreatic islet cells of IRS-2 deficient mice. Pancreatic islets (*arrows*) in a control mouse (**a**) and a diabetic mouse (**b**). Magnification, ×200

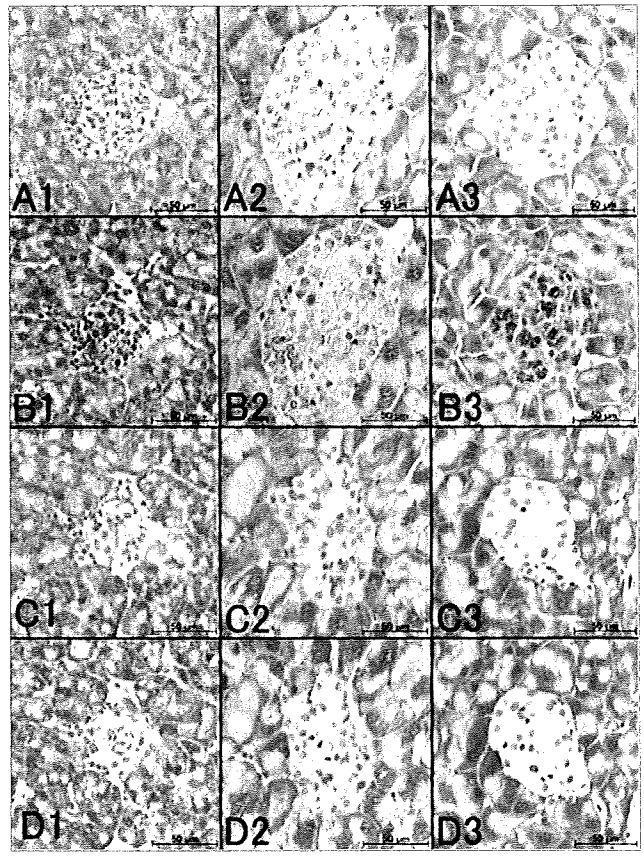

Fig. 2 Observation of islet-associated autoantibodies in serum of NOD and IRS-2 deficient mice. Columns 1, 2 and 3 present diabetic NOD, control IRS2-deficient and diabetic IRS2-deficient mouse pancreatic sections, respectively. Control NOD mouse serum (**A**) reacted with diabetic NOD (**A1**), control IRS2 deficient (**A2**) and diabetic IRS2 deficient mouse (**A3**) pancreatic sections. Diabetic NOD (**B1-3**), control IRS2 (**C1-3**) and diabetic IRS2 (**D1-3**) mouse sera reacted with pancreatic sections, respectively

lower than those of the control mice. Activities of FBPase in gluconeogenesis and malic enzyme in fatty acid synthesis in liver of the diabetic mice were significantly higher than those of the controls. In the mitochondrial fraction of liver of the diabetic mice, activities of 3-HBD were significantly higher than those of the controls, whereas activities of AST and PC were significantly lower than those of the controls. In the liver of the diabetic mice, activities of cytosolic LDH, G6PD, AST and mitochondrial GLDH were lower than those of the control mice (Table 2). On histopathological examination, the pancreatic islets of the diabetic mice were significantly decreased in size and number compared to those of the control mice. In particular, size and number of insulin β cells secreted in the diabetic mice decreased significantly compared to those in the controls, whereas number of glucagon β cells secreted decreased a little. Remarkable insulitis was not observed in pancreatic sections in the diabetic mice (Fig. 1). In the serum of the diabetic NOD mouse, the islet-related antibodies reacted with their own islets (Fig. 2, B1) and IRS2-deficient mouse islets before (Fig. 2, B2) and after (Fig. 2, B3) onset of fulminant diabetes. In the serum of the control NOD mouse without glycosuria, the islet-related antibodies were not observed (Fig. 2, A1-3). In sera of control and diabetic IRS2-deficient mice, the islet-related antibodies were not observed (Fig. 2, C1-3 and D1-3).

Discussion

Fulminant type 1 DM reported by Imagawa and others [10, 11] accounts for 20% of type 1 diabetes in Japan [30] and shows clinical characteristics of (1) remarkably abrupt onset of disease; (2) very short (< 1 week) duration of diabetic symptoms, such as polyuria, thirst and body weight loss; (3) acidosis at diagnosis; (4) negative status of islet-related antibodies, islet cell antibodies (ICA), anti-glutamic acid decarboxylase antibodies (GADAb), insulin autoantibodies (IAA) or anti-islet antigen 2 antibodies (IA-2); (5) virtually no C-peptide secretion (< 10 μg/day in urine); and (6) elevated serum pancreatic enzyme level [10]. In fulminant type 1 diabetes, Fas and Fas ligand expression are lacking and the mechanism of β cell destruction differs from that in autoimmune type 1 DM [31, 32]. However the degradation mechanism of β cells in fulminant type 1 DM of humans is unknown.

The clinical symptoms of fulminant DM observed in only male IRS2-deficient mice are significant increase in plasma glucose and cholesterol concentrations and a significant decrease in plasma IRI and C-peptide concentrations. All the diabetic mice showed reduction of body weight, glycosuria and ketonuria and they were considered to fall into complete insulin deficiency. In the diabetic mice with insulin deficiency, their plasma TG and FFA concentrations were expected to increase generally, however those concentrations were not changed in the IRS2-deficient diabetic mice. In our previous report [9], plasma TG and FFA concentrations decreased significantly notwithstanding plasma glucose and cholesterol concentrations increased significantly in the diabetic IRS2-deficient mice at 14 weeks of age. Liver-specific insulin receptor knockout (LIR-KO) mice with remarkable insulin resistance showed a significant decrease in their plasma TG and FFA concentrations [33]. As IRS2-deficient mice seemed to have a unique regulation mechanism of plasma TG and FFA concentrations, their characteristics in lipid metabolism should be further studied in more IRS2-deficient mice. In conclusion, the clinical characteristics in fulminant diabetic IRS2-deficient mice resembled those in fulminant type 1 DM of humans.

In liver of the diabetic IRS2-deficient mice, activities of enzymes in glycolysis and the malate-aspartate shuttle were significantly depressed, whereas those in gluconeogenesis and ketone body synthesis were significantly elevated. Decreased activities of pyruvate carboxylase, supplying oxaloacetate to the TCA cycle, suggested depression of citrate synthesis, the rate-limiting reaction of the TCA cycle [34, 35], and activation of ketone body synthesis. Moreover, depression in the malate-aspartate shuttle means decreased ATP production [36, 37]. Decrease in glycolysis or increase in gluconeogenesis and ketone body synthesis may be typical metabolic changes induced by complete insulin deficiency. Decreased activities of LDH, MDH, AST and GLDH in the diabetic IRS2-deficient mice reflected depression of liver function frequently observed in the diabetic animals [38]. On the other hand, histopathological examination of pancreas showed prominent atrophy of islets and decreased size and number of β cells, whereas function of α cells was considered to be maintained in the diabetic IRS2-deficient mice. In the diabetic IRS2-deficient mice, hepatic steatosis is frequently observed [9]. The finding of severe, selective destruction of pancreatic β cells was considered to be one of the characteristics in fulminant DM in IRS2-deficient mice. The diabetic IRS2-deficient mice did not show the islet-related antibodies observed in the diabetic NOD mice as autoimmune type 1 DM model. The degradation mechanism of pancreatic islet cells in IRS2-deficient mice may differ clearly from that in the diabetic NOD mice. IRS2-deficient mice develop diabetes because of insulin resistance in the liver and failure to undergo β cell hyperphasia [39]. Progress of changes in islet mass should be studied in the diabetic IRS2-deficient mice to investigate pancreatic β cell destruction. At the moment abrupt increase in plasma glucose concentrations and appearance of ketonuria are available indicators to decide complete insulin deficiency caused by pancreatic β cell destruction in diabetic mice.

In IRS2-deficient mice, the sterol regulatory element-binding protein (SREBP)-1 downstream genes, such as ATP citrate lyase and fatty acid synthase genes, are significantly increased and an excess amount of lipid is accumulated in their tissues [39, 40]. Accumulated lipid is also considered to be one of the causes of injury to their pancreatic islets. As fulminant DM in IRS2-deficient mice resembles human fulminant type 1 DM, IRS2-deficient mice are a good animal model for type 2 DM of humans and some IRS2-deficient mice with fulminant type 1 DM may be a useful animal model for studying the degradation mechanism of pancreatic β cells in progressing to fulminant type 1 DM.

Acknowledgements This work was supported in part by 'Academic Frontier' Project for Private Universities: matching fund subsidy from Ministry of Education, Culture, Sports, Science and Technology of Japan (MEXT), 2005–2009 and Grants-in-Aid for Scientific Research (No. 16380214 to T. Arai and No. 17200029 to Y. Ohnishi) from MEXT.

Conflict of interest The authors declare that they have no conflict of interest related to the publication of this manuscript.

References

1. Tamemoto H, Kadowaki K, Tobe K et al (1994) Insulin resistance and growth in mice lacking insulin receptor substrate-1. Nature 372:182–186
2. Araki E, Lipes MA, Patti ME et al (1994) Alternative pathway of insulin signaling in mice with target disruption of the IRS-1 gene. Nature 372:186–190
3. Suzuki R, Tobe K, Aoyama M et al (2004) Both insulin signaling defects in the liver and obesity contribute to insulin resistance and cause diabetes in Irs2(−/−) mice. J Biol Chem 279:25039–25049
4. Patti ME, Sun XJ, Bruening JC et al (1995) 4PS/insulin receptor substrate (IRS)-2 is the alternative substrate of the insulin receptor in IRS-1-deficient mice. J Biol Chem 270:24670–24673
5. Terauchi Y, Iwamoto K, Tamemoto H et al (1997) Development of non-insulin-dependent diabetes mellitus in the double knockout mice with disruption of insulin receptor substrate-1 and beta cell glucokinase gene. Genetic reconstitution of diabetes as a polygenic disease. J Clin Invest 99:861–866
6. Withers DJ, Burks DJ, Towery H et al (1999) Irs-2 coordinated Igf-1 receptor-mediated beta-cell development and peripheral insulin signaling. Nat Med 23:32–40
7. Kido Y, Burks DJ, Withers DJ et al (2000) Tissue-specific insulin resistance in mice with mutations in the insulin receptors, IRS-1, and IRS-2. J Clin Invest 105:199–205
8. Kubota N, Tobe K, Terauchi Y et al (2000) Disruption of insulin receptor substrate 2 causes type 2 diabetes because of liver insulin resistance and lack of compensatory beta-cell hyperplasia. Diabetes 49:1880–1889
9. Hashimoto H, Arai T, Takeguchi A et al (2006) Ontogenic characteristics of enzyme activities and plasma metabolites in C57BL/6J:Jcl mice deficient in insulin receptor substrate 2. Comp Med 56:176–187
10. Imagawa A, Hanafusa T, Miyagawa J et al (2000) A novel subtype of type 1 diabetes mellitus characterized by a rapid onset and an absence of diabetes-related antibodies. N Engl J Med 342:301–307
11. Imagawa A, Hanafusa T, Miyagawa J et al (2000) A proposal of three distinct subtypes of type 1 diabetes mellitus based on clinical and pathological evidence. Ann Med 32:539–543
12. Imagawa A, Hanafusa T (2006) Fulminant type 1 diabetes mellitus. Endocr J 53:577–584
13. Tsuji A, Torres-Rosado A, Arai T et al (1991) Hepsin, a cell membrane-associated protease. Characterization, tissue distribution, and gene localization. J Biol Chem 266:16948–16953
14. Huggett AG, Nixon DA (1957) Use of glucose oxidase, peroxidase and o-dianisidine in determination of blood and urinary glucose. Lancet 2:368–370
15. Tanaka A, Urabe S, Takeguchi A et al (2006) Comparison of activities of enzymes related to energy metabolism in peripheral leukocytes and livers between Holstein dairy cows and ICR mice. Vet Res Commun 30:29–38
16. Vinuela E, Salas M, Sols A (1963) Glucokinase and hexokinase in liver in relation to glycogen synthesis. J Biol Chem 238:PC1175–PC1177
17. Bergmeyer HU, Gawehn K, Grassl M (1974) Glucose-6-phosphate dehydrogenase from yeast. In: Bergmeyer HU (ed) Methods of enzymatic analysis, Vol 1. Verlag Chemie, New York, pp 458–459
18. Kaloustian HD, Stolzenbach FE, Everse J et al (1969) Lactate dehydrogenase of lobster (Homarus americanus) tail muscle. I. Physical and chemical properties. J Biol Chem 244:2891–2901
19. Bergmeyer HU, Bernt E (1974) Malate dehydrogenase. UV-assay. In: Bergmeyer HU (ed) Methods of enzymatic analysis, Vol 2. Verlag Chemie, New York, pp 613–617
20. Rej R, Horder M (1983) Aspartate aminotransferase (glutamate oxaloacetate transaminase). In: Bergmeyer HU (ed) Methods of enzymatic analysis, 3rd Edn. Verlag Chemie, New York, pp 416–433
21. Jomain-Baum M, Schramm VL, Hanson RW (251) Mechanism of 3-mercaptopicolinic acid inhibition of hepatic phosphoenolpyruvate carboxykinase (GTP). J Biol Chem 251:37–44
22. Latzko E, Gibbs M (1974) Alkaline C1-fructose-1,6-diphosphatase. In: Bergmeyer HU (ed) Methods of enzymatic analysis, Vol 2. Verlag Chemie, New York, pp 881–884
23. Takeda Y, Suzuki F, Inoue H (1969) ATP citrate lyase (citrate cleavage enzyme). In: Lowenstein JM (ed) Methods of enzymology, Vol 13. Academic Press, New York, pp 153–160
24. Martin BB, Denton RM (1970) The intracellular localization of enzymes in white-adipose-tissue fat cells and permeability properties of fat-cell mitochondria. Biochem J 117:861–877
25. Halestrap AP, Denton RM (1973) Insulin and the regulation of adipose tissue acetyl-coenzyme A carboxylase. Biochem J 132:509–517
26. Schmidt E (1974) Glutamate dehydrogenase UV-assay. In: Bergmeyer HU (ed) Methods of enzymatic analysis, Vol 2. Verlag Chemie, New York, pp 650–656
27. Bergmeyer HU, Gawehn K, Grassl M (1974) 3-Hydroxybutyrate dehydrogenase. In: Bergmeyer HU (ed) Methods of enzymatic analysis, Vol 1. Verlag Chemie, New York, pp 475–476
28. Scrutton MC, Olmsted MR, Utter MF (1969) Pyruvate carboxylase from chicken liver. In: Lowenstein JM (ed) Methods in enzymology, Vol 13. Academic Press, New York, pp 235–250
29. Bradford MM (1976) A rapid and sensitive method for the quantitation of microgram quantities of protein utilizing the principle of protein-dye binding. Anal Biochem 72:248–254
30. Imagawa A, Hanafusa T, Uchigata Y et al (2003) Fulminant type 1 diabetes, a nationwide survey in Japan. Diabetes Care 26:2345–2352
31. Sayama K, Imagawa A, Okita K et al (2005) Pancreatic beta and alpha cells are both decreased in patients with fulminant type 1 diabetes: a morphometrical assessment. Diabetologia 48:1560–1564
32. Imagawa A, Hanafusa T, Uchigata Y et al (2005) Different con-

tribution of class II HLA in fulminant and typical autoimmune type 1 diabetes mellitus. Diabetologia 48:294–300
33. Michael MD, Kulkarni RN, Postic C et al (2000) Loss of insulin signaling in hepatocytes leads to severe insulin resistance and progressive hepatic dysfunction. Mol Cell 6:87–97
34. Newsholme P, Gordon S, Newsholme EA (1987) Rates of utilization and fates of glucose, glutamine, pyruvate, fatty acids and ketone bodies by mouse macrophages. Biochem J 242:631–636
35. Otton R, Mendonca JR, Curi R (2002) Diabetes causes marked changes in lymphocyte metabolism. J Endocrinol 174:55–61
36. MacDonald MJ (1982) Evidence of the malate aspartate shuttle in pancreatic islet. Arch Biochem Biophys 213:643–649
37. Matschinsky FM (1996) A lesson in metabolic regulation inspired by the glucokinase sensor paradigm. Diabetes 45:223–241
38. Magori E, Nakamura M, Inoue A et al (2005) Malate dehydrogenase activities are lower in some types of peripheral leucocytes of dogs and cats with type 1 diabetes mellitus. Res Vet Sci 78:39–44
39. Tobe K, Suzuki R, Aoyama M et al (2001) Increased expression of the sterol regulatory element-binding protein-1 gene in insulin receptor substrate-$2^{-/-}$ mouse liver. J Biol Chem 276:38337–38340
40. Taniguchi CM, Ueki K, Kahn CR (2005) Complementary roles of IRS-1 and IRS-2 in the hepatic regulation of metabolism. J Clin Invest 115:718–727

Adiponectin suppresses colorectal carcinogenesis under the high-fat diet condition

T Fujisawa,[1] H Endo,[1] A Tomimoto,[1] M Sugiyama,[1] H Takahashi,[1] S Saito,[1] M Inamori,[1] N Nakajima,[2] M Watanabe,[3] N Kubota,[4] T Yamauchi,[4] T Kadowaki,[4] K Wada,[5] H Nakagama,[6] A Nakajima[1]

► Additional figures and tables are published online only at http://gut.bmj.com/content/vol57/issue11

[1] Division of Gastroenterology, Yokohama City University School of Medicine, Yokohama, Japan; [2] Department of Pathology, National Institute of Infectious Diseases, Tokyo, Japan; [3] Laboratory for Medical Engineering, Graduate School of Engineering, Yokohama National University, Yokohama, Japan; [4] Department of Internal Medicine, Graduate school of Medicine, University of Tokyo, Tokyo, Japan; [5] Department of Pharmacology, Graduate School of Dentistry, Osaka University, Osaka, Japan; [6] Biochemistry Division, National Cancer Center Research Institute, Tokyo, Japan

Correspondence to: Dr A Nakajima, 3-9 Fukuura, Kanazawa-ku, Yokohama 236-0004, Japan; Nakajima-tky@umin.ac.jp

Revised 4 July 2008
Accepted 22 July 2008
Published Online First 1 August 2008

ABSTRACT

Background and aims: The effect of adiponectin on colorectal carcinogenesis has been proposed but not fully investigated. We investigated the effect of adiponectin deficiency on the development of colorectal cancer.

Methods: We generated three types of gene-deficient mice (adiponectin-deficient, adiponectin receptor 1-deficient, and adiponectin receptor 2-deficient) and investigated chemical-induced colon polyp formation and cell proliferation in colon epithelium. Western blot analysis was performed to elucidate the mechanism which affected colorectal carcinogenesis by adiponectin deficiency.

Results: The numbers of colon polyps were significantly increased in adiponectin-deficient mice compared with wild-type mice fed a high-fat diet. However, no difference was observed between wild-type and adiponectin-deficient mice fed a basal diet. A significant increase in cell proliferative activity was also observed in the colonic epithelium of the adiponectin-deficient mice when compared with wild-type mice fed a high-fat diet; however, no difference was observed between wild-type and adiponectin-deficient mice fed a basal diet. Similarly, an increase in epithelial cell proliferation was observed in adiponectin receptor 1-deficient mice, but not in adiponectin receptor 2-deficient mice. Western blot analysis revealed activation of mammalian target of rapamycin, p70 S6 kinase, S6 protein and inactivation of AMP-activated protein kinase in the colon epithelium of adiponectin-deficient mice fed with high-fat diet.

Conclusions: Adiponectin suppresses colonic epithelial proliferation via inhibition of the mammalian target of the rapamycin pathway under a high-fat diet, but not under a basal diet. These studies indicate a novel mechanism of suppression of colorectal carcinogenesis induced by a Western-style high-fat diet.

Adipose tissue produces and secretes several bioactive substances[1 2] known as adipocytokines,[3] and obesity is an important risk factor for many human diseases, including colorectal cancer and diabetes mellitus.[4 5] Several case–control studies have shown that high-fat diets may promote the development of colorectal cancer,[6] and the results of animal experiments suggest the existence of a link between fat intake and colorectal cancer[7]. Adiponectin is mainly secreted by adipocytes[8] and is a key hormone responsible for insulin sensitisation.[9 10] While adiponectin protein is abundantly found in the plasma of healthy human subjects,[11] adiponectin mRNA levels in the adipose tissue and plasma are dramatically decreased in patients with obesity and/or type 2 diabetes mellitus.[12–15] Because both obesity and type 2 diabetes have been reported to be associated with an elevated risk of colorectal cancer,[14–16] we hypothesised that the plasma level of adiponectin may be related to the risk of colorectal cancer.

Several contradictory results have been reported from human clinical studies on the relationship between the plasma levels of adiponectin and the risk of colorectal cancer.[17 18] While some clinical studies have been conducted in humans, no studies investigating the relationship between the plasma levels of adiponectin and the risk of colorectal cancer have been reported in animal models. Therefore, the mechanism underlying the promotion of colorectal carcinogenesis by adiponectin deficiency still remains unclear.

It is now well known that the adiponectin receptor exists in two isoforms: adiponectin receptor 1 (AdipoR1), which is abundantly expressed in the skeletal muscle; and adiponectin receptor 2 (AdipoR2), which is predominantly expressed in the liver.[19] These receptors mediate the enhanced activation of AMP-activated protein kinase (AMPK) and the peroxisome proliferator-activated receptor α (PPARα), as well as the increase in fatty-acid oxidation and glucose uptake induced by adiponectin.[20 21]

Recently, involvement of the AMPK/mammalian target of rapamycin (mTOR) pathway in the development of various types of cancer has attracted attention.[22–24] The important role of mTOR in mammalian cells is related to its control of mRNA translation. The targets for mTOR signalling are proteins involved in controlling the translational machinery, including the ribosomal protein S6 kinases and S6 proteins that regulate the initiation and elongation phases of translation.[25 26] With regard to the upstream control, mTOR is regulated by signalling pathways linked to several oncoproteins or tumour suppressors, including AMP-activated protein kinase (AMPK).[25 27] mTOR is located at the intersection of major signalling pathways and is believed to be capable of integrating a large panel of stress signals, including nutrient deprivation, energy depletion, and oxidative or hypoxic stresses. In particular, AMPK activation has been reported to directly inhibit mTOR[28] and suppress cell proliferation.

Using adiponectin-deficient mice (KO) we therefore investigated whether adiponectin deficiency might promote the development of colorectal cancer, and examined the involvement of the AMPK/mTOR pathway in the effect of adiponectin on colon carcinogenesis.

Table 1 Histological findings of azoxymethane-induced colon polyps in adiponectin-deficient (KO) mice and wild-type (WT) mice receiving a high-fat diet

Experimental group	Adenocarcinoma	Adenoma	Total
WT (n = 10)	15 (42%)	21 (58%)	36 (100%)
KO (n = 10)	51 (60%)	34 (40%)	85 (100%)

MATERIALS AND METHODS

Animal models

All mice were treated humanely in accordance with the National Institutes of Health and AERI-BBRI Animal Care and Use Committee guidelines. Adiponectin (ACRP30 or AdipoQ)-deficient (*ACRP30−/−*) mice (KO mice) and adiponectin receptor 1 or 2-deficient mice (*AdipoR1−/−* or *AdipoR2−/−*) were generated by our group as described previously.[21] We performed the experiments in this study using littermate mice backcrossed to C57Bl/6 for 10 generations.

The animals were fed a basal diet or a high-fat diet until the end of the study. The composition of both diets is listed in supplementary table 1. Three to five mice were housed per metallic cage with sterilised softwood chips as bedding, in a barrier-sustained animal room air-conditioned at 24 (SD 2)°C and 55% humidity, under a 12 h light–dark cycle.

Induction of colon polyps

Azoxymethane (AOM) was purchased from Sigma (St. Louis, Missouri, USA). Mice (6 weeks old) were divided into four groups: (1) WT mice fed the basal diet (n = 10), (2) KO mice fed the basal diet (n = 10), (3) WT mice fed the high-fat diet (n = 10), and (4) KO mice fed the high-fat diet (n = 10). Mice were injected intraperitoneally with 10 mg/kg of AOM once a week for 6 weeks and sacrificed at 20 weeks following initiation of AOM injection to evaluate the difference in the extent of polyp formation between the KO and WT mice (supplementary fig 1A).

Induction of aberrant crypt foci

Mice (6 weeks old) were divided into four groups: (1) WT mice fed the basal diet (n = 12 mice), (2) KO mice fed the basal diet (n = 11), (3) WT mice fed the high-fat diet (n = 11), and (4) KO mice fed the high-fat diet (n = 11). Mice were given two weekly intraperitoneal injections of 10 mg/kg of AOM and sacrificed at 6 weeks following initiation of AOM injection (supplementary fig 1B). The protocol of the 2-amino-1-methyl-6-phenylimidazo-[4,5-*b*]pyridine (PhIP)-induced aberrant crypt foci (ACF) model is shown in supplementary fig 2A.[39]

Effect of the AMP kinase activator and mTOR inhibitor on colon carcinogenesis

The AMP kinase activator 5-aminoimidazole-4-carboxamide-l-β-D-ribofuranoside (AICAR) and the mTOR inhibitor rapamycin were purchased from BIOMOL (Plymouth Meeting, PA, USA). WT and KO mice (6 weeks old) were intraperitoneally injected with AICAR (0.1 mg/kg/day), rapamycin (0.2, 0.4, 0.8 mg/kg) or vehicle (saline) until the end of the experiment. The mice in each group were fed the high-fat diet and received AOM injections according to the ACF protocol.

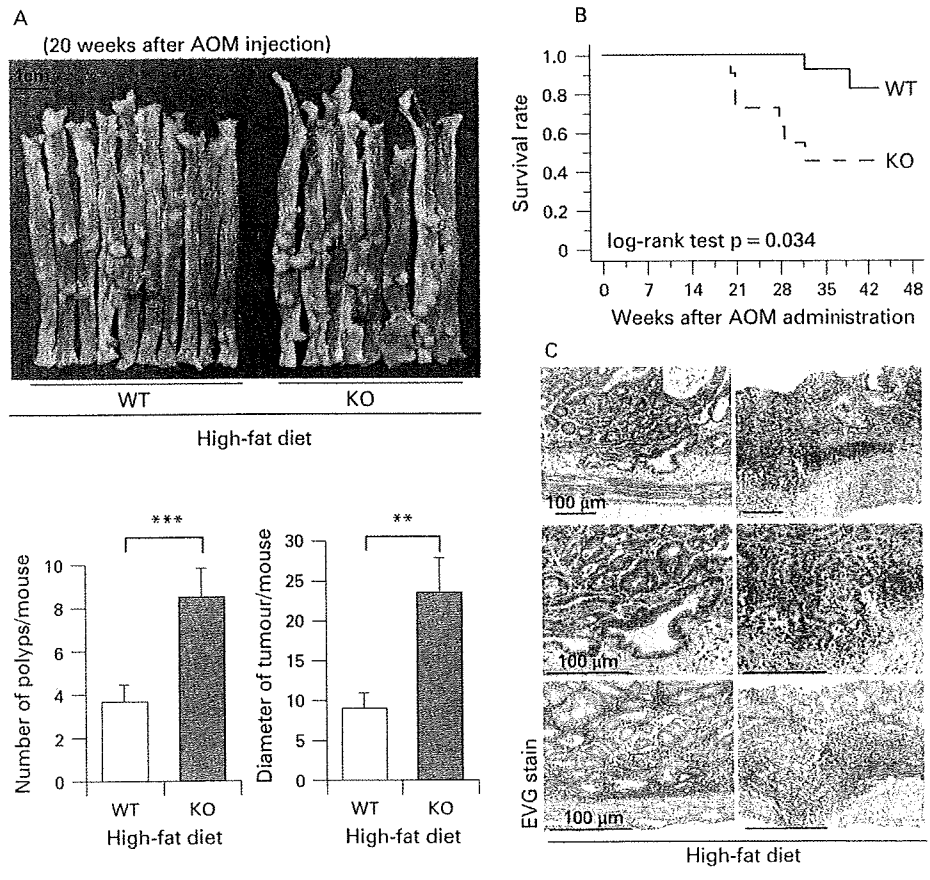

Figure 1 Promotion of colon polyp formation in adiponectin-deficient (KO) mice under the high-fat diet condition. (A) Upper panel: Macroscopic findings of colon polyp in wild-type (WT) and KO littermate mice under the high-fat diet condition at 20 weeks following initiation of azoxymethane (AOM) injection. Lower panel: Number and diameter of polyps per mouse in the high-fat diet groups. Each column represents the mean (with the SEM), *p<0.05. (B) Survival rate of the WT and KO littermates under the high-fat diet condition. The survival rate of the WT mice (solid line) was significantly higher than that of the KO mice (broken line) under the high-fat diet condition. More than half of the KO mice died by the end of the study, while only two of the WT mice died. (C) Invasive polyps in the colons obtained from the KO mice under the high-fat diet condition. Haematoxylin and eosin staining (upper and middle panels) and Elastica van Gieson staining (EVG stain, lower panel) were performed using samples isolated from three individual animals.

Gut 2008;**57**:1531–1538. doi:10.1136/gut.2008.159293

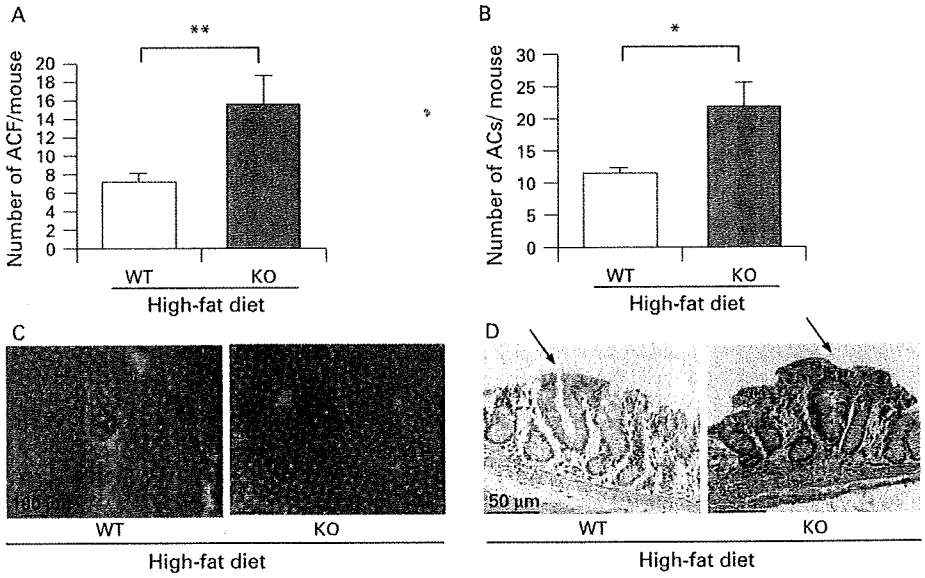

Figure 2 Enhancement of the formation of aberrant crypt foci (ACF) in adiponectin-deficient (KO) mice under the high-fat diet condition. (A,B) Average number of ACF (A) and aberrant crypts (ACs) (B) in the two groups, wild-type (WT) and KO littermate mice, under the high-fat condition, respectively. Each column represents the mean (with the SEM), *p<0.05, **p<0.01. (C) Stereomicroscopic observations of ACF in colon tissue from each group. The samples were stained with 0.2% methylene blue. (D) Representative haematoxylin and eosin staining of ACF in WT and KO mice under the high-fat diet condition.

Histological analysis of the aberrant crypt foci and colon polyps

The entire colon was removed and fixed in 10% neutralised formalin and the numbers of polyps, ACF and aberrant crypts (ACs) were counted as described previously.[30] To facilitate counting, the colons were stained with 0.2% methylene blue solution and observed by stereomicroscopy. After being counted, they were removed and embedded in paraffin blocks according to standard procedures. Paraffin sections were then prepared at 3.0 μm thickness, stained with hematoxylin & eosin and Elastica van Gieson staining for a detection of submucosal invasion, and subjected to histological analysis.

Analysis of the survival rate

In the polyp induction experiment, both the KO (n = 11) and WT (n = 12) mouse groups were continuously observed for 45 weeks. Survival curves were drawn using the Kaplan–Meier method and analysed using the log-rank test.

Assay for assessment of the proliferative activity of the colon epithelial cells

We evaluated the bromodeoxyuridine (BrdU) and the proliferating cell nuclear antigen (PCNA) labelling indices to determine the proliferative activity of the colon epithelial cells. BrdU (BD Biosciences, New Jersey, USA) was diluted in phosphate-buffered saline at 1 mg/ml and administered intraperitoneally at a dose of 50 mg/kg, 1 h prior to the sacrifice of the mice. Immunohistochemical detection of BrdU was performed using a commercial kit (BD Biosciences) and a PCNA detection kit (Zymed Laboratories, South San Francisco, California, USA) was used for PCNA detection. The BrdU and PCNA labelling indices were expressed as the ratio of the number of positively stained nuclei to the total number of nuclei counted in the crypts of the colon. The criteria for selecting the crypts included the presence of a clearly visible and continuous cell column on each side of the crypt. Twenty crypts were evaluated each mouse.

Immunoblotting

The extracted protein was separated by sodium dodecyl sulfate polyacrylamide gel electrophoresis (SDS-PAGE) and the separated proteins were transferred to a polyvinylidene difluoride (PVDF) membrane (Amersham, London, UK). The membranes were probed with primary antibodies specific for adiponectin receptor 1, adiponectin receptor 2 (Santa Cruz Biotech, California, USA), phospho-AMPK, AMPK, phospho-mTOR, mTOR, phospho-S6K, S6K, phospho-S6 protein, S6 protein (Cell Signaling Technology, Danvers, Massachusetts, USA) and glyceraldehyde-3-phosphate dehydrogenase (GAPDH) (Trevigen, Gaithersburg, Maryland, USA). Horseradish-peroxidase-conjugated secondary antibodies and the enhanced chemiluminescence (ECL) detection kit (Amersham) were used for the detection of specific proteins.

Statistical analysis

Statistical analyses for the number of ACF, number of colon polyps, BrdU labelling index and PCNA labelling index were conducted using the Mann–Whitney test. The results for western blot analysis were obtained using the Student t test. Values of $p<0.05$ were regarded as denoting statistical significance.

RESULTS

Promotion of colon polyp formation and lower survival rate in adiponectin-deficient mice under the high-fat diet

The number of polyps in the KO mice was significantly higher than that in the WT mice under the high-fat diet (fig 1A), while there was no difference in the total number of polyps between the WT and KO mice under the basal diet (supplementary fig 3). The sum of the diameter of the polyps per mouse was also measured and similar results were obtained. Table 1 shows histological findings of polyps in mice under high-fat diet. We also observed the survival rate of the WT and KO mice under the high-fat diet condition in the AOM model, and there was a significantly higher survival rate in the WT mice than in the KO mice. While more than half of the KO mice were dead by the end of the study, only two WT mice died (fig 1B).

Interestingly, invasion by malignant cells was observed in parts of the polyps exclusively in the KO mice under the high-fat diet, and the malignant cells were found to have destroyed the muscularis mucosae and invaded the submucosal layer in

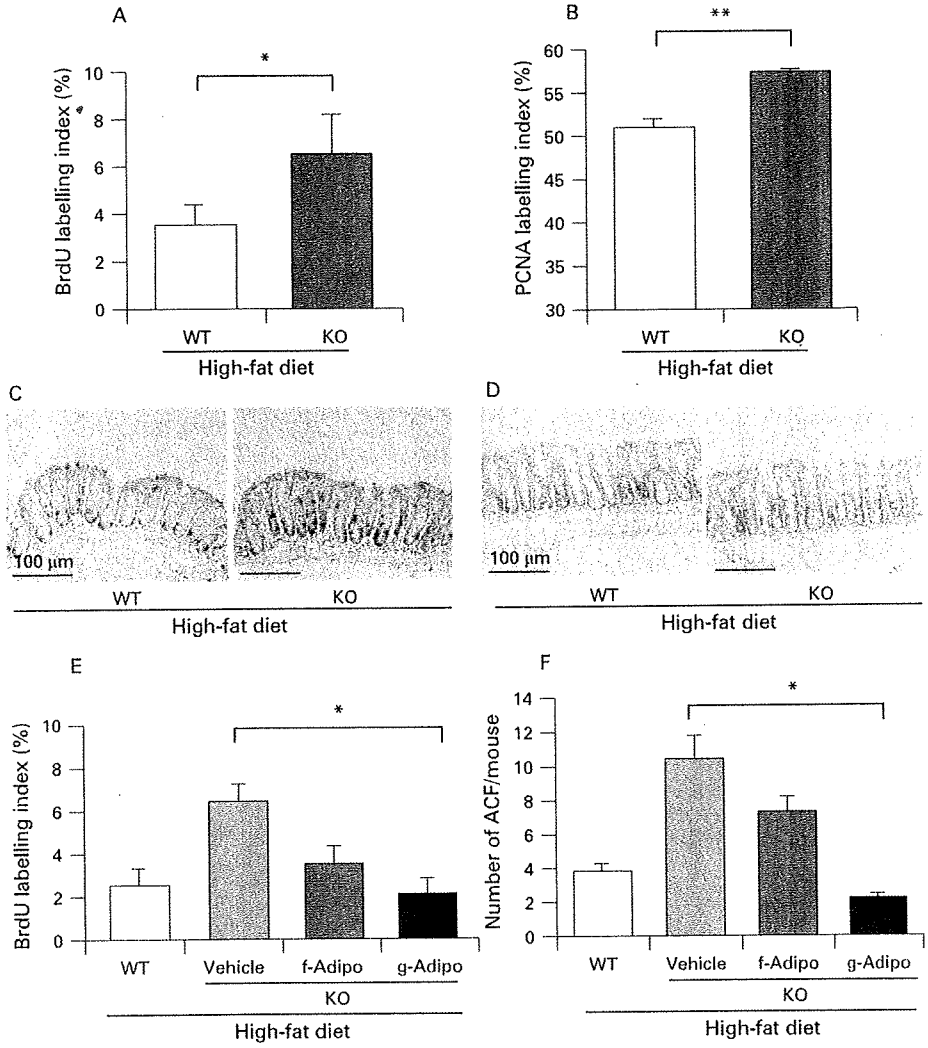

Figure 3 Increase in the colonic epithelial cell proliferative activity in adiponectin-deficient (KO) mice under the high-fat diet condition. (A,B) Average bromodeoxyuridine (BrdU) labelling index (A) and proliferating cell nuclear antigen (PCNA) labelling index (B) in each group in the aberrant crypt foci (ACF) formation experiment. BrdU was administered intraperitoneally 1 h prior to the sacrifice of the animals. Both indices were expressed as the percentage of positively stained nuclei out of the total number of nuclei counted in the crypts of the colon. Each bar represents the mean (with the SEM), *$p<0.05$, **$p<0.01$. (C,D) Representative immunohistochemical staining for BrdU (C) and PCNA (D) in each group. (E,F) Wild-type (WT) mice and KO littermate mice fed the high-fat diet were injected intraperitoneally with 50 μg/body recombinant full-length adiponectin (f-Adipo) or 5 μg/body recombinant globular adiponectin domain (g-Adipo) or only vehicle every other day for 6 weeks in an ACF experiment. Adiponectin ameliorates the epithelial cell hyperproliferation in the KO mice under the high-fat diet condition (E). The same effect was observed on the suppression of ACF formation (F).

the tissue specimens (fig 1C), whereas no such invasion was observed in the WT mice. At the end of experiment, the body weight in KO mice was decreased compared to WT mice under the high-fat diet (supplementary fig 4A,B).

Enhanced formation of aberrant crypt foci in adiponectin-deficient mice under the high-fat diet

To investigate the effect of adiponectin in suppressing colon carcinogenesis under the high-fat diet, we analysed colon specimens for the formation of ACF, defined as clusters of aberrant crypts, as a marker of the early stage of colorectal carcinogenesis.[51 52] Although there were no significant differences in the total number of ACF and ACs between the WT and KO littermates mice under the basal diet (data not shown), the numbers of ACF and ACs in the KO mice were significantly higher than those in the WT littermates under the high-fat diet (fig 2A,B). The macroscopic and microscopic characteristics of the ACF in the WT and KO mice under the high-fat diet condition are shown in fig 2C,D; no morphological differences of the ACF were observed between the WT and the KO mice. The differences in the body weight (supplementary fig 4C,D) and the serum levels of adiponectin, glucose, insulin, lipids, and tumour necrosis factor α between the WT and the KO mice are shown in supplementary table 2. In agreement with previous metabolic studies of adiponectin-deficient mice,[35] there were no differences between the two groups under the high-fat diet. To confirm the protective role of adiponectin in colorectal carcinogenesis, the food-borne carcinogen PhIP was used as a second model of colon carcinogenesis in mice fed a high-fat diet. Similar results to those obtained using the AOM-induced carcinogenesis model was obtained (supplementary fig 2).

Increase in cell proliferative activity in adiponectin-deficient mice under the high-fat diet condition

We investigated the proliferative activity of the colon epithelium by determining the BrdU and PCNA labelling indices. Both indices were increased in the KO mice as compared with their WT littermates under the high-fat diet (fig 3A–D). On the other hand, there was no difference under the basal diet (data not shown). Moreover, we examined both indices in colon polyps under the high-fat diet but there was no difference between WT and KO mice (supplementary fig 5).

Adiponectin ameliorates epithelial cell hyper-proliferation in adiponectin-deficient mice under the high-fat diet condition

We administered recombinant adiponectin via an intraperitoneal injection to KO mice in comparison to their WT littermates under the high-fat diet condition. Globular domain adiponectin

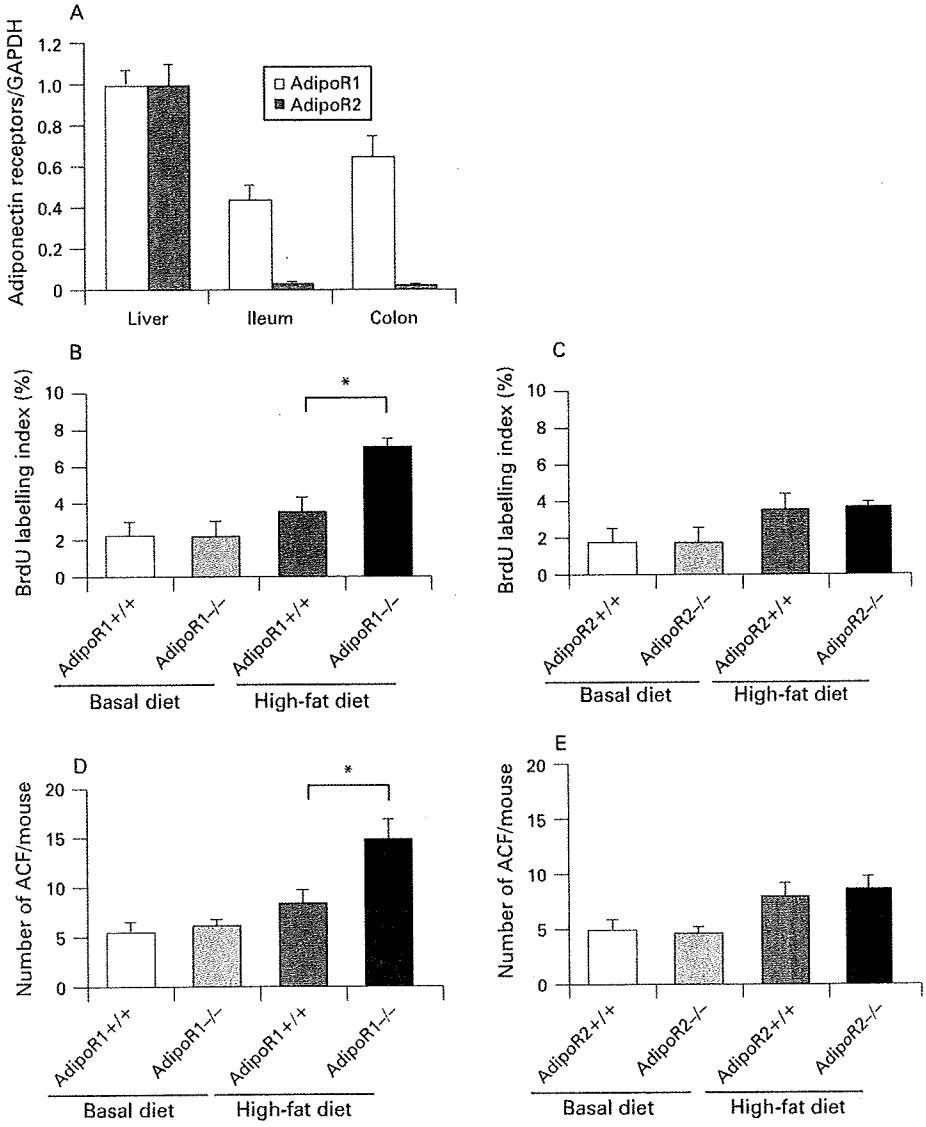

Figure 4 Expression of the adiponectin receptors AdipoR1 and AdipoR2 in the liver, ileum and colon, and promotion of epithelial cell proliferation in AdipoR1−/− mice under high-fat diet condition. (A) Western blot analysis to investigate the expression of AdipoR1 and AdipoR2 was performed on protein obtained from the liver, ileum and colon. The ratio in the liver was defined as 1.0. (B,C): Average bromodeoxyuridine (BrdU) labelling index on colon epithelium from AdipoR1−/− and AdipoR2−/− mice in comparison to the wild-type (WT) littermate mice under basal and high-fat diet condition. The increase in the epithelial cell proliferation was observed in AdipoR1−/− mice, but not in AdipoR2−/− mice under the high-fat diet condition. (D,E) Average number of aberrant crypt foci (ACF) in AdipoR1−/− (D) and AdipoR2−/− mice (E). GADPH, glyceraldehyde-3-phosphate dehydrogenase.

exerted a more potent effect on the suppression of proliferative activity of colon epithelial cells than full-length adiponectin under the high-fat diet (fig 3E). The same effect was observed on the suppression of ACF formation (fig 3F).

The increase in cell proliferative activity in adiponectin receptor 1-deficient mice under the high-fat diet

By using western blot analyses we investigated whether adiponectin receptors are expressed in the colon epithelium, and observed that AdipoR1 was predominantly expressed in the colon in comparison to AdipoR2 (fig 4A).

The BrdU index in the *AdipoR1*−/− mice was significantly higher than in their WT littermates under the high-fat diet (fig 4B). The numbers of ACF and ACs in the *AdipoR1*−/− mice were also significantly higher than their WT littermates (fig 4D). However, no difference in BrdU index and the number of ACF was observed in *AdipoR2*−/− mice and their WT littermates (fig 4C,E). These results suggest that the AdipoR1-mediated, but not the AdipoR2-mediated, pathway may play an important role in the suppressive effect of adiponectin on colorectal carcinogenesis under the high-fat diet, not under the basal diet.

The mTOR pathway is relatively activated in the colon epithelium of adiponectin-deficient mice in comparison to wild-type mice under the high-fat diet

In order to clarify the mechanisms underlying the enhanced proliferative activity of the colon epithelial cells in the presence of adiponectin deficiency, we investigated the expression levels of various potential target proteins in colonic specimens prepared from the WT mice and KO mice under the high-fat diet. The results of western blot analysis revealed that the amounts of phosphorylated mTOR, S6 kinase and S6 protein were significantly higher in the KO mice compared with the WT mice under the high-fat diet (fig 5B–D). It has been reported that adiponectin activates AMPK via AdipoR1, and AMPK is known to suppress the mTOR pathway.[20 54] A significant decrease in the level of phosphorylated AMPK was observed in the KO mice compared with that in the WT mice under the high-fat diet (fig 5A). Moreover, adiponectin administration ameliorated activation of the AMPK/mTOR pathway in KO mice under the high-fat diet condition (supplementary fig 6). These results indicate that, under the high-fat diet, deficiency of adiponectin suppresses AMPK activation, which results in

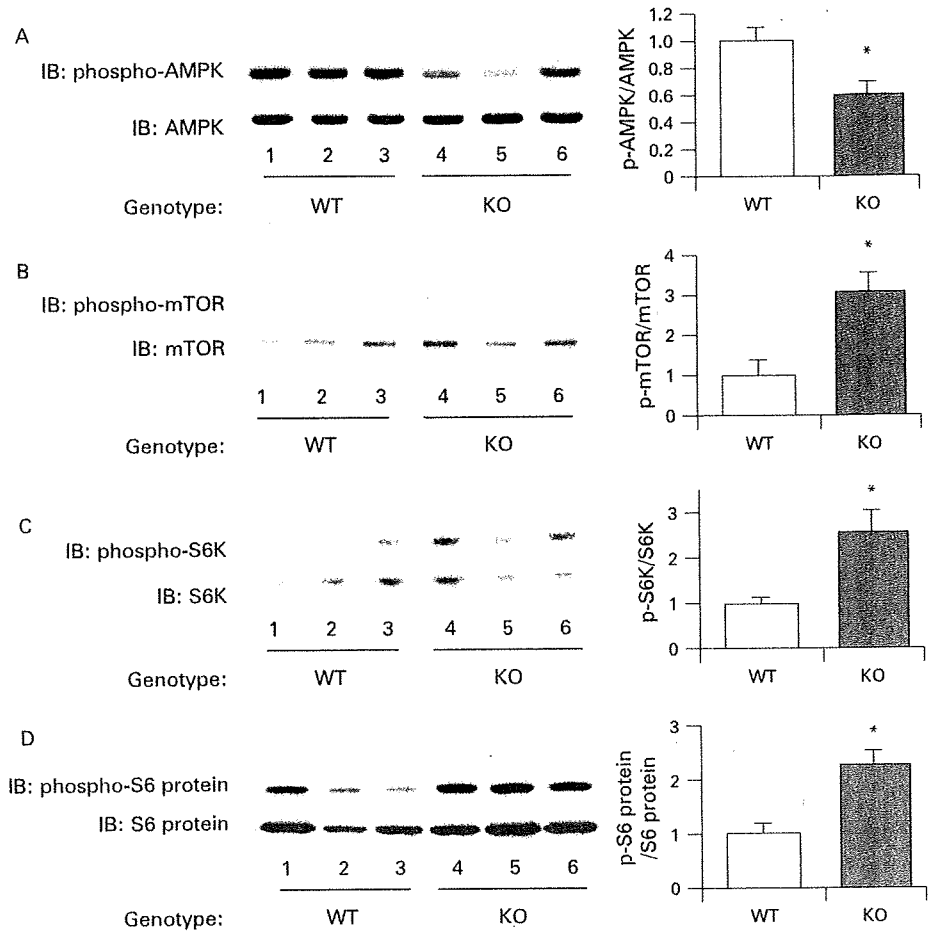

Figure 5 Activation of the mammalian target of rapamycin (mTOR) pathway in adiponectin-deficient (KO) mice compared with that in wild-type (WT) mice under the high-fat diet condition. Western blot analysis for phosphorylated and total AMP-activated protein kinase (AMPK) (A), mTOR (B), p70 S6 kinase (C) and S6 protein (D) in the colon from the WT and KO mice under the high-fat diet condition. Left panels: Pictures of the western blotting. Right panels: Graphs showing the ratios of the phosphorylated protein to the total protein. Each column represents the mean (with the SEM), *$p<0.05$.

activation of the mTOR pathway directly involved in cell proliferation. To confirm whether adiponectin actually suppresses the AMPK/mTOR pathway, we treated mice with the specific AMPK activator AICAR, or the mTOR inhibitor rapamycin. The increase of cell proliferation in the colon epithelium was significantly suppressed by AICAR in the KO mice under the high-fat diet, but no effect in WT mice under high-fat diet (fig 6A,B). Similarly, ACF formation was significantly suppressed by AICAR in the KO mice under the high-fat diet, but not in the WT mice (fig 6C). In the KO mice under the high-fat diet, treatment with rapamycin significantly reduced the BrdU index in a dose dependent manner and ACF formation (fig 6D,E). These results indicate that the activation of the mTOR pathway may play important roles in the increase in epithelial cell proliferation in KO mice under the high-fat diet, and may play an important role in the promotion of colon carcinogenesis in KO mice under the high-fat diet condition.

DISCUSSION

The existence of a relationship between high-fat diets and colorectal cancer has been speculated for a long time, but no definitive conclusions have been arrived at yet.[55] It has been reported that the secretion of adiponectin from adipocytes is suppressed in obese humans.[11] Considered together with the knowledge that obesity is also an important risk factor for colorectal cancer,[4] we speculated that adiponectin might suppress the development of colorectal cancer.

We demonstrated significantly enhanced formation of polyps and ACF in the KO mice compared with that in the WT mice under the high-fat diet. Furthermore, an increase in proliferative activity of colonic epithelial cells was also observed in the KO mice under the high-fat diet, but not under the basal diet. These results suggest that under the high-fat diet, but not under basal diet, a deficiency of adiponectin significantly promotes the proliferative activity of the colonic epithelial cells, and thereby may be promoting colorectal carcinogenesis. We demonstrated that the AdipoR1 is predominantly expressed in colon epithelium. The increase in the proliferative activity of the colonic epithelial cells and the number of ACF were observed in AdipoR1−/− mice, not in the AdipoR2−/− mice, under high-fat diet condition. These results suggest that the AdipoR1-mediated, but not the AdipoR2-mediated, pathway may play an important role in the suppressive effect of adiponectin on the increased in epithelial cell proliferation under the high-fat diet.

We demonstrated the activation of the mTOR pathway and inactivation of AMPK in colon epithelial cells in the KO mice under the high-fat diet, but there was no difference under the basal diet (data not shown). Moreover, the replacement of adiponectin ameliorated the activated mTOR pathway by adiponectin deficiency. AICAR, the AMPK specific activator, suppressed the increase in epithelial cell proliferation in KO mice, but not in WT littermates, under high-fat diet. Furthermore, rapamycin, an mTOR inhibitor, also significantly suppressed the increase in epithelial cell proliferation only in KO mice under high-fat diet in a dose dependent manner,

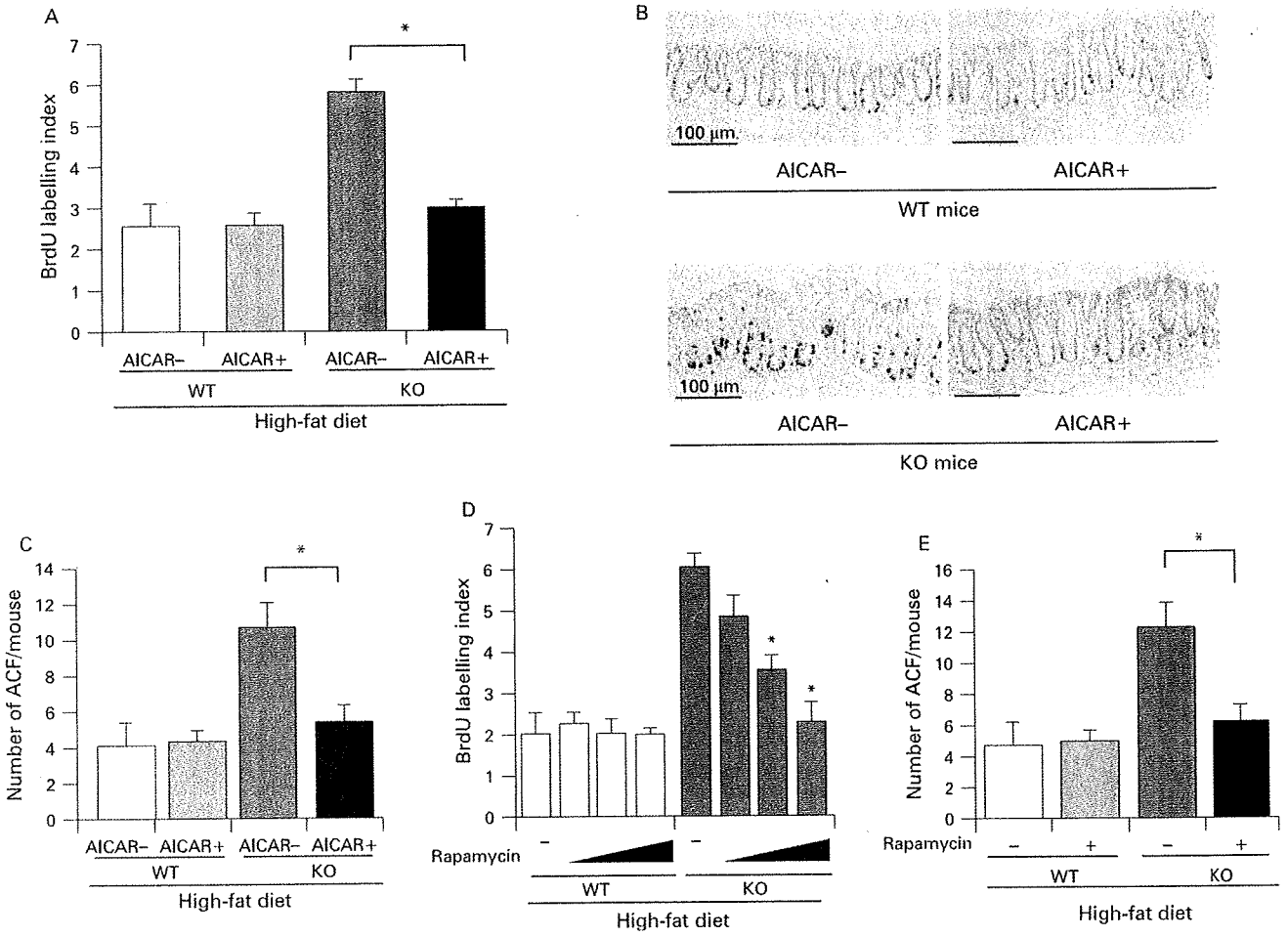

Figure 6 Suppression of epithelial cell hyper-proliferation by activation of AMP-activated protein kinase (AMPK) or by inhibition of the mammalian target of rapamycin (mTOR) in adiponectin-deficient (KO) mice under the high-fat diet condition. Wild-type (WT) mice (6 weeks old) were injected intraperitoneally with the AMPK activator 5-aminoimidazole-4-carboxamide-l-β-D-ribofuranoside (AICAR) (0.1 mg/kg/day), or vehicle until the end of the experiment. Mice in the high-fat diet group were also given two weekly intraperitoneal injections of 10 mg/kg of azoxymethane (AOM). (A) Average bromodeoxyuridine (BrdU) labelling index in the WT and KO mice treated (+) or not treated (−) with AICAR under the high fat diet condition. BrdU was administered intraperitoneally 1 h prior to the sacrifice of the animals. Each column represents the mean (with the SEM), *$p<0.05$. (B) Representative immunohistochemical staining patterns for BrdU in each group. (C) Average number of aberrant crypt foci (ACF) in the WT and KO mice treated (+) or not treated (−) with AICAR under the high fat diet condition. (D) WT and KO mice fed the high-fat (HF) diet were injected intraperitoneally with various doses of rapamycin (0.2, 0.4, 0.8 mg/kg) or only with vehicle every other day for 6 weeks. Average values of the BrdU index were decreased in the KO mice in a dose dependent manner, but not in the WT mice. *$p<0.05$ compared to non-treated KO mice. (E) Average number of ACF in the WT and KO mice treated (+) or not treated (−) with rapamycin (0.8 mg/kg) under the high fat diet condition. Each bar represents the mean (with the SEM), *$p<0.05$.

suggesting that mTOR plays an important role in promoting epithelial cell proliferation where there is a lack of adiponectin under a high-fat diet. It has been reported that AMPK directly inhibits mTOR.[25] Therefore we speculate that the AMPK/mTOR pathway is a possible mechanism closely involved in the protective effect of adiponectin in colon carcinogenesis under the high-fat diet (supplementary fig 7). Concerning other major pathways in the carcinogenesis, it was reported that adiponectin attenuated the adenomatous polyposis coli (APC)/β-catenin pathway,[26] and increased p53 expression[27] in different kinds of cancer cells. p53 also suppresses the mTOR pathway through activation of phosphatase and tensin homologue deleted on chromosome ten (PTEN), AMPK, insulin-like growth factor-1-binding protein 3 (IGF1-BP3) and tuberous sclerosis complex-2 (TSC-2).[28] Although the mechanism underlying the promotion of colon carcinogenesis by a high-fat diet is still unknown, our present data strongly suggest that plasma adiponectin derived from adipocytes suppresses the mTOR pathway through the activation of AMPK, resulting in suppression of the cell proliferative activity and, thereby, suppression of colon carcinogenesis, under the high-fat diet. However, in the event of a decrease in plasma adiponectin level, AMPK activity is suppressed, resulting in the activation of mTOR and the members downstream in the pathway, such as the p70 S6 kinase and S6 protein. We speculate that activation of the mTOR pathway directly promotes colonic epithelial cell proliferation and, thereby, colorectal carcinogenesis.

It has been reported that the plasma adiponectin levels are decreased in humans under the conditions of obesity and/or diabetes mellitus.[11] However, it was reported that plasma levels of adiponectin in the mice are not decreased in response to high-fat feeding for several weeks.[29] Therefore, we used

adiponectin-deficient mice to elucidate the role of adiponectin on colonic epithelial proliferation and carcinogenesis under the high-fat diet. Our experimental condition in which we used adiponectin-deficient mice fed a high-fat diet may well have reflected these pathophysiological conditions in humans.

The purpose of our study was to elucidate the role of adiponectin on colon carcinogenesis, not to elucidate the mechanism whereby a high-fat diet promotes carcinogenesis. This mechanism remains unknown. However, we could provide a possible mechanism underlying the protective roles of adiponectin in colorectal carcinogenesis promoted by a high-fat diet We consider that AMPK and mTOR may be novel therapeutic targets for the prevention of colorectal cancer under the low levels of plasma adiponectin in an obese population where the obesity is a result of a Western-style diet with a high fat content. Our results shed light on a novel mechanism by which adiponectin might suppress carcinogenesis mediated by a high-fat diet. Continued investigation to elucidate the precise mechanisms involved is necessary because of the major clinical implications.

Acknowledgements: We thank M Ochiai and M Hiraga for technical assistance.

Funding: This work was supported in part by a Grant-in-Aid for research on the Third Term Comprehensive Control Research for Cancer from the Ministry of Health, Labour and Welfare, Japan to AN; a grant from the National Institute of Biomedical Innovation (NBIO) to AN; a grant from the Ministry of Education, Culture, Sports, Science and Technology, Japan (KIBAN-B) to AN; and a research grant of the Princess Takamatsu Cancer Research Fund.

Competing interests: None.

Ethics approval: All animal experiments were approved by the institutional Animal Care and Use Committee of Yokohama City University School of Medicine.

REFERENCES

1. **Friedman JM.** Obesity in the new millennium. *Nature* 2000;**404**:632–4.
2. **Berg AH,** Combs TP, Schere PE. ACRP30/adiponectin: an adipokine regulating glucose and lipid metabolism. *Trends Endocrinol Metab* 2002;**13**:84–9.
3. **Shimomura I,** Funahashi T, Takahashi M, *et al.* Enhanced expression of PAI-1 in visceral fat: possible contributor to vascular disease in obesity. *Nature Med* 1996;**2**:800–3.
4. **Bianchini F,** Kaaks R, Vainio H. Overweight, obesity and cancer risk. *Lancet Oncol* 2002;**3**:565–74.
5. **Calle EE,** Rodriguez C, Walker-Thurmond K, *et al.* Overweight, obesity and mortality from cancer in a prospectively studied cohort of U.S. adults. *N Engl J Med* 2003;**348**:1625–38.
6. **Giovannucci E,** Goldin B. The role of fat, fatty acids, and total energy intake in the etiology of human colon cancer. *Am J Clin Nutr* 1997;**66**:1564S–71S.
7. **Reddy BS.** Dietary fat and colon cancer: animal model studies. *Lipids* 1992;**27**:807–13.
8. **Delporte ML,** El Mkadem SA, Quisquater M, *et al.* Leptin treatment markedly increased plasma adiponectin but barely decreased plasma resistin of *ob/ob* mice. *Am J Physiol Endocrinol Metab* 2004;**287**:E446–53.
9. **Yamauchi T,** Kamon J, Waki H, *et al.* The fat-derived hormone adiponectin reverses insulin resistance associated with both lipoatrophy and obesity. *Nature Med* 2001;**7**:941–46.
10. **Berg AH,** Combs TP, Du X, *et al.* The adipocyte-secreted protein Acrp30 enhances hepatic insulin action. *Nature Med* 2001;**7**:947–53.
11. **Arita Y,** Kihara S, Ouchi N, *et al.* Paradoxical decrease of an adipose-specific protein, adiponectin, in obesity. *Biochem Biophys Res Commun* 1999;**257**:79–83.
12. **Halleux CM,** Takahashi M, Delporte ML, *et al.* Secretion of adiponectin and regulation of apM1 gene expression in human visceral adipose tissue. *Biochem Biophys Res Commun* 2001;**288**:1102–7.
13. **Hotta K,** Funahashi T, Arita Y, *et al.* Plasma concentrations of a novel, adipose-specific protein, adiponectin, in type 2 diabetic patients. *Arterioscler Thromb Vasc Biol* 2000;**20**:1595–9.
14. **Giovannucci E,** Ascherio A, Rimm EB, *et al.* Physical activity, obesity, and risk for colon cancer and adenoma in men. *Ann Intern Med* 1995;**122**:327–34.
15. **Schoen RE,** Tangen CM, Kuller LH, *et al.* Increased blood glucose and insulin, body size, and incident colorectal cancer. *J Natl Cancer Inst* 1999;**91**:1147–54.
16. **Giovannucci E.** Insulin, insulin-like growth factors and colon cancer: a review of the evidence. *J Nutr* 2001;**131**:3109S–20S.
17. **Wei EK,** Giovannucci E, Fuchs CS, *et al.* Low plasma adiponectin levels and risk of colorectal cancer in men: a prospective study. *J Natl Cancer Inst* 2005;**97**:1688–94.
18. **Likanova A.** Serum adiponectin is not associated with risk of colorectal cancer. *Cancer Epidemiol Biomarkers Prev* 2006;**15**:401–2.
19. **Yamauchi T,** Kamon J, Ito Y, *et al.* Cloning of adiponectin receptors that mediate antidiabetic metabolic effects. *Nature* 2003;**423**:762–9.
20. **Yamauchi T,** Kamon J, Minokoshi Y, *et al.* Adiponectin stimulates glucose utilization and fatty-acid oxidation by activating AMP-activated protein kinase. *Nature Med* 2002;**8**:1288–95.
21. **Yamauchi T,** Nio Y, Maki T, *et al.* Targeted disruption of AdipoR1 and AdipoR2 causes abrogation of adiponectin binding and metabolic actions. *Nature Med* 2007;**13**:332–9.
22. **Averous J,** Proud CG. When translation meets transformation: the mTOR story. *Oncogene* 2006;**25**:6423–35.
23. **Guertin DA,** Sabatini DM. An expanding role for mTOR in cancer. *Trends Mol Med* 2005;**11**:353–61.
24. **Wullschleger S,** Loewith R, Hall MN. TOR signaling in growth and metabolism. *Cell* 2006;**124**:471–84.
25. **Avruch J,** Belham C, Weng Q, *et al.* The p70 S6 kinase integrates nutrient and growth signals to control translational capacity. *Prog Mol Subcell Biol* 2001;**26**:115–54.
26. **Sahin F,** Kannangai R, Adegbola O, *et al.* mTOR and p70 S6 kinase expression in primary liver neoplasms. *Clin Cancer Res* 2004;**10**:8421–5.
27. **Corradetti MN,** Guan KL. Upstream of the mammalian target of rapamycin: do all roads pass through mTOR? *Oncogene* 2006;**25**:6347–60.
28. **Luo Z,** Saha AK, Xiang X, *et al.* AMPK, the metabolic syndrome and cancer. *Trends Pharmacol Sci* 2005;**26**:69–76.
29. **Nakagama H,** Nakanishi N, Ochiai M. Modeling human colon cancer in rodents using a food-borne carcinogen, PhIP. *Cancer Sci* 2005;**96**:627–36.
30. **Osawa E,** Nakajima A, Wada K, *et al.* Peroxisome proliferator-activated receptor γ ligans suppress colon carcinogenesis induced by azoxymethane in mice. *Gastroenterology* 2003;**124**:361–7.
31. **McLellan EA,** Bird RP. Aberrant crypts: potential preneoplastic lesions in the murine colon. *Cancer Res* 1998;**48**:6187–92.
32. **Konstantakos AK,** Siu IM, Pretlow TG, *et al.* Human aberrant crypt foci with carcinoma in situ from a patient with sporadic colon cancer. *Gastroenterology* 1996;**111**:772–7.
33. **Nawrocki AR,** Rajala MW, Tomas E, *et al.* Mice lacking adiponectin show decreased hepatic insulin sensitivity and reduced responsiveness to peroxisome proliferator-activated receptor gamma agonists. *J Biol Chem* 2006;**281**:2554–60.
34. **Tomas E,** Tsao TS, Saha AK, *et al.* Enhanced muscle fat oxidation and glucose transport by ACRP30 globular domain: Acetyl-CoA carboxylase inhibition and AMP-activated protein kinase activation. *Proc Natl Acad Sci USA* 2002;**99**:16309–13.
35. **Zock PL.** Dietary fats and cancer. *Curr Opin Lipidol* 2001;**12**:5–10.
36. **Wang Y,** Lam JB, Lam KS, *et al.* Adiponectin modulates the glycogen synthase kinase-3beta/beta-catenin signaling pathway and attenuates mammary tumorigenesis of MDA-MB-231 cells in nude mice. *Cancer Res* 2006;**66**:11462–70.
37. **Mistry T,** Digby JE, Desai KM, *et al.* Leptin and adiponectin interact in the regulation of prostate cancer cell growth via modulation of p53 and bcl-2 expression. *Br J Urol Int* 2008;**101**:1317–22.
38. **Feng Z,** Hu W, Rajagopal G, *et al.* The tumor suppressor p53: cancer and aging. *Cell Cycle* 2008;**7**:842–7.
39. **Bullen JW Jr,** Bluher S, Kelesidis T, *et al.* Regulation of adiponectin and its receptors in response to development of diet-induced obesity in mice. *Am J Physiol Endocrinol Metab* 2007;**292**:E1079–86.

Am J Physiol Endocrinol Metab 296: E47–E55, 2009.
First published October 21, 2008; doi:10.1152/ajpendo.90690.2008.

α_2-AMPK activity is not essential for an increase in fatty acid oxidation during low-intensity exercise

Shinji Miura,[1] Yuko Kai,[1] Yasutomi Kamei,[1,3] Clinton R. Bruce,[4] Naoto Kubota,[2,5] Mark A. Febbraio,[4] Takashi Kadowaki,[2,5] and Osamu Ezaki[1]

[1]Nutritional Science Program and [2]Clinical Nutrition Program, National Institute of Health and Nutrition; [3]Department of Molecular Medicine and Metabolism, Medical Research Institute, Tokyo Medical and Dental University, Tokyo, Japan; [4]Cellular and Molecular Metabolism Laboratory, Baker IDI Heart and Diabetes Institute, Melbourne, Australia; and [5]Department of Metabolic Diseases, Graduate School of Medicine, University of Tokyo, Tokyo, Japan

Submitted 13 August 2008; accepted in final form 11 October 2008

Miura S, Kai Y, Kamei Y, Bruce CR, Kubota N, Febbraio MA, Kadowaki T, Ezaki O. α_2-AMPK activity is not essential for an increase in fatty acid oxidation during low-intensity exercise. *Am J Physiol Endocrinol Metab* 296: E47–E55, 2009. First published October 21, 2008; doi:10.1152/ajpendo.90690.2008.—A single bout of exercise increases glucose uptake and fatty acid oxidation in skeletal muscle, with a corresponding activation of AMP-activated protein kinase (AMPK). While the exercise-induced increase in glucose uptake is partly due to activation of AMPK, it is unclear whether the increase of fatty acid oxidation is dependent on activation of AMPK. To examine this, transgenic mice were produced expressing a dominant-negative (DN) mutant of α_1-AMPK (α_1-AMPK-DN) in skeletal muscle and subjected to treadmill running. α_1-AMPK-DN mice exhibited a 50% reduction in α_1-AMPK activity and almost complete loss of α_2-AMPK activity in skeletal muscle compared with wild-type littermates (WT). The fasting-induced decrease in respiratory quotient (RQ) ratio and reduced body weight were similar in both groups. In contrast with WT mice, α_1-AMPK-DN mice could not perform high-intensity (30 m/min) treadmill exercise, although their response to low-intensity (10 m/min) treadmill exercise was not compromised. Changes in oxygen consumption and the RQ ratio during sedentary and low-intensity exercise were not different between α_1-AMPK-DN and WT. Importantly, at low-intensity exercise, increased fatty acid oxidation in response to exercise in soleus (type I, slow twitch muscle) or extensor digitorum longus muscle (type II, fast twitch muscle) was not impaired in α_1-AMPK-DN mice, indicating that α_1-AMPK-DN mice utilize fatty acid in the same manner as WT mice during low-intensity exercise. These findings suggest that an increased α_2-AMPK activity is not essential for increased skeletal muscle fatty acid oxidation during endurance exercise.

adenosine 5′-monophosphate-activated protein kinase; fasting; respiratory quotient ratio; fatty acid oxidation; mitochondria; 5-aminoimidazole-4-carboxamide-1-β-D-ribofuranoside

AN ACUTE BOUT OF EXERCISE increases skeletal muscle glucose uptake by translocating the intracellular glucose transporter 4 (GLUT4) to the plasma membrane (10, 14) and increases fatty acid oxidation by stimulating carnitine palmitoyl transferase 1 (CPT1) activity, which limits fatty acid transport into mitochondria (33, 41). Both steps may be mediated by activation of AMP-activated protein kinase (AMPK), a sensor of fuel levels in skeletal muscle (15). AMPK is a heterotrimer composed of an α (α_1 and α_2)-catalytic subunit and β (β_1 and β_2)- and γ (γ_1, γ_2, and γ_3)-noncatalytic subunits. Of the 12 possible subunit combinations, only 3 exist in human skeletal muscle, namely $\alpha_1/\beta_2/\gamma_1$, $\alpha_2/\beta_2/\gamma_1$, and $\alpha_2/\beta_2/\gamma_3$ (4). Expression of γ_3 is predominately restricted to glycolytic skeletal muscle [type II, i.e., extensor digitorum longus (EDL); Ref. 24]. It is expressed at very low levels in oxidative muscles (type I, i.e., soleus). The roles of α_1, α_2, and γ_3 in skeletal muscles for glucose metabolism during muscle contraction (or exercise) have been extensively studied; however, the importance of AMPK activity in regulating fatty acid oxidation during exercise is unclear.

Mice expressing a dominant-negative (DN) AMPK transgene in skeletal muscle and α_1- and α_2-knockout mice have been produced (13, 19, 20, 28, 37), and the role of AMPK on contraction-induced glucose uptake has been investigated. Mu et al. (28) reported that glucose transport activity in soleus and EDL from α_2-AMPK-DN mice after in situ electrical contraction was only 30% less than that in wild-type (WT) mice. Fujii et al. (13) produced α_1- and α_2-AMPK-DN transgenic mice and found that these transgenic mice showed the same phenotype in which α_2-activity in skeletal muscle was barely detectable and α_1 activity was partially reduced. Contraction-stimulated glucose transport in isolated EDL, tibialis anterior, or gastrocnemius was normal in α_2-AMPK-DN transgenic mice (13). In addition, when force production during contraction ex vivo was matched between WT littermates and α_2-AMPK-DN mice, a similar increase in contraction-induced glucose transport was observed in isolated EDL from both groups of mice (13). In whole body α_1- and α_2-knockout mice, glucose transport activity in electrically stimulated (100-Hz, 0.2-ms impulse for 10 min), isolated soleus and EDL from either α_1- or α_2-AMPK knockout subgroups was not impaired. This suggests that the two α-isoforms can compensate for each other in terms of contraction-induced glucose uptake or that neither α-isoform is involved in contraction-induced glucose uptake (19). These studies used tetanic stimulation, a relatively strong electrical stimulation. However, increases in isoform specific AMPK activity differed by mode of electrical stimulation (36). In ex vivo experiments (in isolated EDL), electrical twitch contraction (1 and 2 Hz, 0.1 ms for 2 min) activated α_1-AMPK but not α_2-AMPK, whereas tetanic contraction (100-Hz, train duration = 10 s, 10 min) activated both α_1-AMPK and α_2-AMPK activities (36). Both twitch and tetanic contractions could increase glucose uptake in EDL (36). Recently, it was reported (17) that increased glucose transport in response to

Address for reprint requests and other correspondence: S. Miura, or O. Ezaki, Nutritional Science Program, National Institute of Health and Nutrition, 1-23-1, Toyama, Shinjuku-ku, Tokyo 162-8636, Japan (e-mail: shinjim@nih.go.jp or ezaki@nih.go.jp).

The costs of publication of this article were defrayed in part by the payment of page charges. The article must therefore be hereby marked "*advertisement*" in accordance with 18 U.S.C. Section 1734 solely to indicate this fact.

electrical twitch contraction was not observed in α_1-AMPK knockout mice, suggesting that α_1-AMPK activity is required for stimulation of glucose uptake by twitch contraction. However, it is unknown whether low-intensity twitch contraction ex vivo is relevant to low-intensity exercise in vivo. We could find only one study (3) to examine the effects of exercise. After a swim bout, EDL muscles were excised from AMPK mutant-overexpression *Tg-Prkag3*^{225Q} (dominant-positive mutation) mice, AMPK γ_3-knockout mice, and WT mice and incubated for 20 min to determine the rate of glucose uptake after exercise (3). Swimming increased glucose uptake to an equal extent in all genotypes. These findings strongly suggest that additional pathways mediate contraction (or exercise)-induced glucose uptake.

Conflicting results have been reported regarding exercise-induced fatty acid oxidation. The role of AMPK in contraction-induced fatty acid oxidation has been estimated with the use of an activator of AMPK, 5-aminoimidazole-4-carboxamide-1-β-D-ribofuranoside (AICAR). Like exercise, AICAR leads to phosphorylation of acetyl-CoA carboxylase 2 (ACC2), a major isoform of ACC in skeletal muscle, which decreases malonyl-CoA levels, releasing the inhibition of uptake of fatty acids into mitochondria via CPT1 and thereby stimulating fatty acid oxidation (26). In cardiac myocytes, AICAR induced translocation of fatty acid translocase (FAT)/CD36 to the sarcolemma, leading to enhanced rates of long-chain fatty acid uptake (23). However, it is not clear whether the effects of AICAR-induced increase in fatty acid oxidation are mediated solely by AMPK activation. EDL muscles were excised from AMPK mutant-overexpression *Tg-Prkag3*^{225Q} mice, AMPK γ_3 knockout mice, and WT mice after a swim bout and incubated for 2 h to determine the rate of oleate oxidation after exercise (3). Under these ex vivo conditions, similar rates of oleate oxidation were observed among genotypes.

In this study, we sought to examine the role of AMPK activation on fatty acid oxidation during exercise by generating transgenic mice overexpressing a DN form of the α_1-AMPK subunit in skeletal muscle. We hypothesized that the exercise-induced increase in fatty acid oxidation would be somewhat dependent on activation of AMPK.

METHODS

Transgenic mice. The human α-skeletal actin promoter was used to drive skeletal muscle-specific expression of a DN mutant (D157A) rat α_1-AMPK subunit transgene (6, 27). A complete rat α_1-AMPK (GenBank Accession No. NM019142) cDNA was obtained by PCR of first-strand cDNA from rat skeletal muscle total RNA and subcloned into pCR2.1-TOPO (Invitrogen, Carlsbad, CA). Forward and reverse primer sequences were 5′-CGGAATTCATGGCCGAGAAGCA-GAAGCACGAC-3′ and 5′-ATAAGAATGCGGCCGCTTACTGTG-CAAGAATTTT-3′, respectively. In vitro mutagenesis (Quick Change site-directed mutagenesis kit; Stratagene, La Jolla, CA) was used to change residue Asp 157 to Ala. Asp 157 lies in the conserved DFG motif (subdomain VII in the protein kinase catalytic subunit), which is essential for Mg^{2+} ATP binding in all protein kinases (18, 35). It is reported that coexpression of this mutant with β_1 and γ_1 in CCL13 cells yields a catalytically inactive complex (35) and that an α_1-AMPK-DN mutant inhibits α_2-catalytic activity in COS7 cells (11), rat hepatocytes (44), and mouse skeletal muscles (13). The oligonucleotides used were 5′-GAATGCAAAGATAGCCGCCT-TCGGTCTTTCAAAC-3′ and 5′-GTTTGAAAGACCGAAGGCG-GCTATCTTTGCATTC-3′. The α_1-AMPK (D157A) cDNA released from pCR2.1-TOPO by *Eco*RI and *Not*I digestion was subcloned into human α-skeletal actin promoter plasmids. The nucleotide sequence of the α_1-AMPK (D157A) cDNA was confirmed by sequencing. The transgene construct contains nucleotides (nt) −2,000 to +200 of the human α-skeletal actin promoter, the 1,647-bp complete rat α_1-AMPK (D157A) cDNA, and a polyadenylation signal that is encoded by the bovine growth hormone gene. The purified transgene fragment digested with *Sna*BI and *Sph*I was microinjected into BDF1 mouse eggs at Japan SLC (Hamamatsu, Japan). Two integration-positive mouse lines, C and E, were studied. Male chimeras harboring the α_1-AMPK (D157A) transgene were mated with C57BL/6J females to obtain F1 offspring. The heterozygous F1 male offspring from this breeding were then crossed with purebred C57BL/6J females to obtain heterozygous F2 offspring, and this process was continued until the heterozygous F3 generation of mice was obtained. Heterozygous α_1-AMPK-DN mice and their WT littermates were compared.

Mice were exposed to a cycle of 12-h light (0700-1900) and 12-h darkness (1900-0700) and maintained at a constant temperature of 22°C. The mice were fed a normal chow diet (CE2; CLEA Japan, Tokyo, Japan) ad libitum. All animal procedures were reviewed and approved by the National Institute of Health and Nutrition Ethics Committee on Animal Research.

Western blot. The AMPK protein level in gastrocnemius was measured by Western blotting with anti-α_1, -α_2 (cat. no. 07-350 and 07-363, respectively; Upstate Biotechnology, Lake Placid, NY), -β_1 (cat. no. 4182; Cell Signaling Technology, Beverly, MA), -β_2 (cat. no. sc-20164; Santa Cruz Biotechnology, Santa Cruz, CA), -γ_1 (cat. no. 4187; Cell Signaling Technology), -γ_2 (cat. no. 2536; Cell Signaling Technology), and -γ_3 (cat. no. sc-19145; Santa Cruz Biotechnology)-AMPK antibodies. Phosphorylated and total acetyl-CoA carboxylase (ACC) protein was measured by Western blotting with anti-phospho ACC (S79) antibody (cat. no. 07-303; Upstate Biotechnology) and anti-ACC antibody (cat. no. 3662; Cell Signaling Technology), respectively.

Measurement of AMPK activity. Isoform-specific AMPK (α_1 and α_2) activity was measured as described previously (5) with antibodies against the α_1- or α_2-catalytic subunits of AMPK (cat. no. 07-350 and 07-363, respectively; Upstate Biotechnology) and Dynabeads Protein G (Dynal Biotech ASA, Oslo, Norway).

Measurement of oxygen consumption and carbon dioxide production. Open-circuit indirect calorimetry was performed with an O_2/CO_2 metabolism measuring system for small animals (MK-5000RQ; Muromachi Kikai, Tokyo, Japan). The system monitored $\dot{V}O_2$ and $\dot{V}CO_2$ at 3-min intervals and calculated the respiratory quotient (RQ) ratio ($\dot{V}CO_2/\dot{V}O_2$). To measure energy expenditure and spontaneous motor activity when sedentary, mice were individually placed in the chamber equipped with Supermex (Muromachi Kikai) at 1630 with an adequate amount of normal chow diet. The measurements of energy expenditure under ad libitum conditions were performed from 1900 to 0700 for the dark period and from 0700 to 1630 for the light period.

During fasting experiments, the remaining food was removed at 1700 and the measurements were performed while the animals were fasting from 1900 to 0700 (dark conditions) and from 0700 to 1630 (light conditions).

For the exercise experiments, mice were allowed to acclimatize to the air-tight treadmill chamber (Muromachi Kikai) for 30 min, at which point $\dot{V}O_2$ and $\dot{V}CO_2$ were stable, and measurements were continued for another 30 min while mice were in a sedentary state. Mice were then exercised for 30 min at a speed of 10 m/min (low-intensity exercise).

The substrate utilization rate and energy production rate were calculated using the formula used by Ferrannini (12) where the rate of glucose oxidation (g/min) = 4.55 $\dot{V}CO_2$ (l/min) − 3.21 $\dot{V}O_2$ (l/min) − 2.87 N (mg/min), the rate of lipid oxidation (g/min) = 1.67 ($\dot{V}O_2$ − $\dot{V}CO_2$) − 1.92 N, and the rate of energy production (kcal/min) = 3.91 $\dot{V}O_2$ + 1.10 $\dot{V}CO_2$ − 3.34 N, where N is the rate of urinary nitrogen excretion used to estimate protein oxidation. However, considering

that only a small portion of resting and exercise energy expenditure arises from protein oxidation (40), the contributions of protein oxidation were neglected.

Palmitate oxidation in isolated muscle. To examine palmitate oxidation in muscles, soleus and EDL muscles were dissected tendon to tendon and placed in a 20-ml glass reaction vial containing 2 ml of warmed (30°C), pregassed (95% O_2-5% CO_2, pH 7.4), modified Krebs-Henseleit buffer containing 4% FA-free BSA (Sigma Chemical, St. Louis, MO), 5 mM glucose, and 0.5 mM palmitate, giving a palmitate-to-BSA molar ratio of 1:1. After a 30-min preincubation period, muscle strips were transferred to vials containing 0.5 μCi/ml [1-^{14}C]palmitate (GE Healthcare Life Sciences, Buckinghamshire, UK) for 60 min. During this phase, exogenous palmitate oxidation was monitored by the production of $^{14}CO_2$ (7).

Glycogen measurement. Muscle glycogen content was measured as glycosyl units after acid hydrolysis (22).

AICAR, glucose, and insulin tolerance tests. For the AICAR tolerance test, AICAR (Toronto Research Chemicals, Toronto, Canada) was injected intraperitoneally (250 μg/g body wt) into fed mice. Blood glucose levels were measured at 0, 15, 30, 60, and 90 min after AICAR injection. For the oral glucose tolerance test, D-glucose [1 mg/g body wt, 10% (wt/vol) glucose solution] was administered via a stomach tube after an overnight fast. For the insulin tolerance test, human insulin (Humulin R; Eli Lilly Japan K.K., Kobe, Japan) was injected intraperitoneally (0.75 mU/g body wt) into fed animals. Blood samples were obtained by cutting the tail tip. Blood glucose concentration was measured with a glucose analyzer (Glucometer DEx; Bayer Medical, Tokyo, Japan).

Statistical analysis. Data were analyzed by one-way or two-way ANOVA. Where differences were significant, each group was compared with the other by Student's *t*-test (StatView 5.0; Abacus Concepts, Berkeley, CA). AICAR tolerance is plotted with respect to time and compared by two-way repeated measures ANOVA (StatView 5.0). In the exercise tolerance test, a Kaplan-Meier survival curve was obtained, and the comparison of groups was performed using the log-rank test. Statistical significance was defined as $P < 0.05$. Values are shown as means ± SE.

RESULTS

Production of α_1-AMPK-DN mice. α_1-AMPK-DN mice were made with a DNA construct containing the 5′-flanking skeletal muscle-specific regulatory region and promoter of the human α-skeletal actin gene and a cDNA encoding a DN mutant of α_1-AMPK (Fig. 1*A*). To examine whether overexpression of α_1-AMPK-DN impairs AMPK activity in skeletal muscle, isoform-specific AMPK (α_1 and α_2) activity in skeletal muscle was measured (Fig. 1*B*). α_1-AMPK activities were 58 and 36% lower in lines C and E, respectively, than in WT

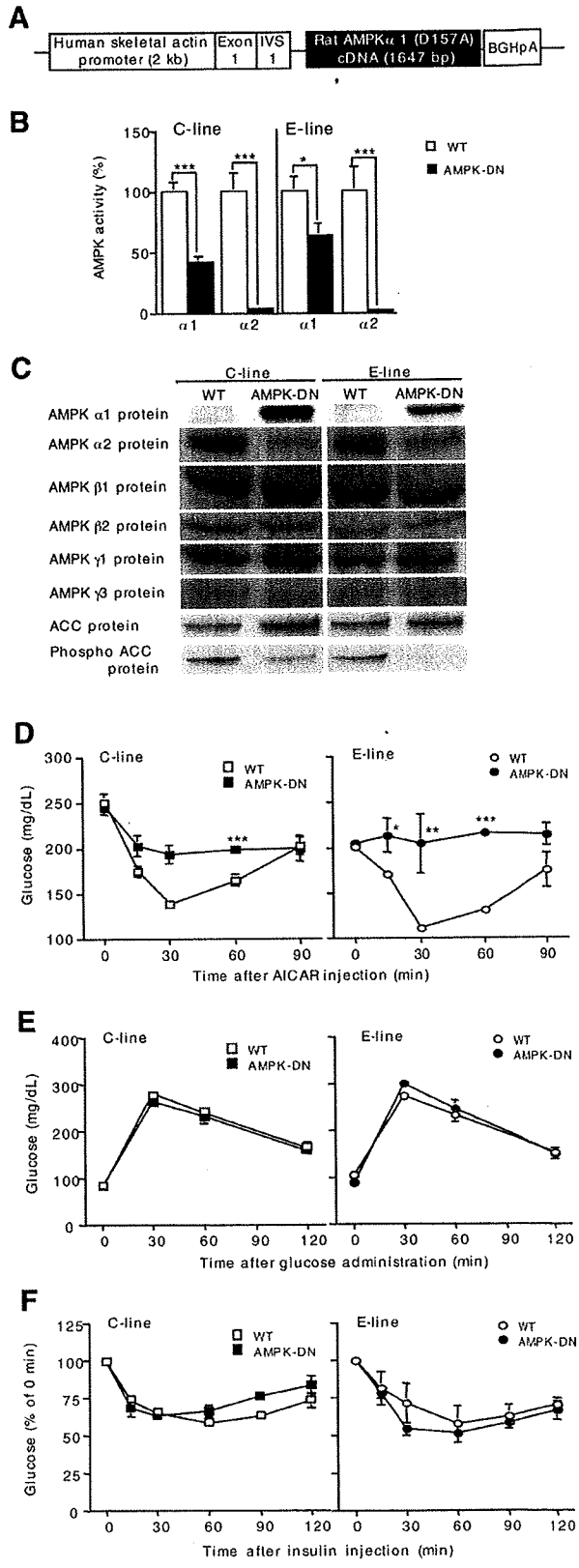

Fig. 1. Generation of transgenic mice with skeletal muscle-specific overexpression of a dominant-negative (DN) form of α_1-AMP-activated protein kinase (AMPK) (D157A). *A*: map of the DN α_1-AMPK (D157A) transgene construct used for microinjection of fertilized eggs. *B*: activities of the α_1- and α_2-AMPK subunits in skeletal muscle (gastrocnemius) from lines C and E transgenic mice and wild-type (WT) littermates. AMPK activity was measured in immunoprecipitates. Values, expressed as a percentage of values in WT littermates, are means ± SE of 4 mice from the C line (12 wk old) and 3 mice from the E line (15 wk old). $^*P < 0.05$; $^{***}P < 0.001$ vs. WT littermates. *C*: typical data of Western blot analyses of AMPK isoforms, acetyl-CoA carboxylase (ACC), and phosphorylated ACC in skeletal muscle (gastrocnemius) from α_1-AMPK-DN (lines C and E) mice and WT littermates. *D*: 5-aminoimidazole-4-carboxamide-1-β-D-ribofuranoside (AICAR) tolerance tests. *E*: oral glucose tolerance tests. *F*: insulin tolerance tests. $^*P < 0.05$; $^{**}P < 0.01$; $^{***}P < 0.001$ vs. WT mice. Data are means ± SE of 3–4 mice. Male mice were used at 8 and 14 wk of age for line C and line E, respectively. For some data points, error bars are smaller than symbols.

littermates, and α_2 activities were reduced by 98 and 99%, respectively. Inhibition of α_2 activity in α_1-AMPK-DN mice corresponded with that previously reported (13). Liver AMPK activity was not altered in α_1-AMPK-DN mice (data not shown). Immunoblot analysis with an isoform-specific anti-α_1-AMPK antibody showed that endogenous α_1-AMPK protein in gastrocnemius was very low in WT littermates, whereas the level of the same size α_1-AMPK protein was markedly increased in α_1-AMPK-DN mice (Fig. 1*C*). Although this antibody did not distinguish between the endogenous and mutated α_1-AMPK protein, these data suggested that almost all endogenous α_1-protein was replaced by mutant α_1-AMPK in α_1-AMPK-DN mice. The amount of the 63-kDa α_2-AMPK protein was decreased by 50–60% in α_1-AMPK-DN mice, which is in agreement with the results of previous studies (13, 44). The α_2-AMPK protein might be degraded, possibly due to the lack of association with β- and γ-isoforms. The levels of other isoforms of AMPK, β_1, β_2, γ_1, and γ_3, were not altered in α_1-AMPK-DN mice. The γ_2 isoform was undetectable (data not shown). Phosphorylated ACC protein levels in α_1-AMPK-DN mice were over 60% lower than those in WT littermates (Fig. 1*C*), suggesting that overexpression of α_1-AMPK-DN impairs AMPK activity and subsequent phosphorylation of ACC in skeletal muscle. However, ACC protein in α_1-AMPK-DN mice (both lines of mice) was ~1.5-fold larger than that in WT littermates ($P < 0.05$; $n = 4$ in each line of mice). The mechanism behind this is not clear. Injection of AICAR, an activator of AMPK, reduces blood glucose levels (15). In previous studies, α_2-AMPK-DN mice (13, 28) and α_2-AMPK-knockout mice (20) were resistant to the effects of AICAR. As expected, α_1-AMPK-DN mice were resistant to AICAR stimulation (Fig. 1*D*), indicating that AICAR-mediated activation of AMPK in skeletal muscle was severely impaired in α_1-AMPK-DN mice. However, abnormalities were not seen in the glucose and insulin tolerance curve of α_1-AMPK-DN mice (Figs. 1, *E* and *F*).

Indirect calorimetry under ad libitum feeding. To examine whether substrate utilization was altered in α_1-AMPK-DN mice, α_1-AMPK-DN (line C) mice and WT littermates were subjected to measurements of oxygen consumption and RQ ratio in sedentary mice fed ad libitum (Fig. 2). The oxygen consumption (Fig. 2*A*, *left*) and RQ ratio (Fig. 2*B*, *left*) were not different between α_1-AMPK-DN mice and WT littermates during the dark cycle (feeding period) and the light cycle (sleeping period). Spontaneous motor activity was reduced during the sleeping period in both groups of mice, but it was not altered between α_1-AMPK-DN and WT littermates (Fig. 2*C*, *left*).

Indirect calorimetry under fasting condition. Fasting reduces glucose oxidation in skeletal muscles and predominates fat oxidation (8). Fasting might uncover a possible abnormality in the fatty acid oxidation by α_1-AMPK-DN mice. Mice were fasted, and their oxygen consumption and RQ ratio were measured during the dark cycle and the light cycle (Fig. 2, *A*, *B*, and *C*, *right*). Oxygen consumption and RQ ratio during fasting were reduced in both groups of mice, compared with ad libitum feeding, but there was no discernable difference between both groups of mice. Body weights were reduced similarly between the two groups after 24-h fasting. These data suggested that α_2-AMPK also did not affect the fatty acid oxidation during fasting.

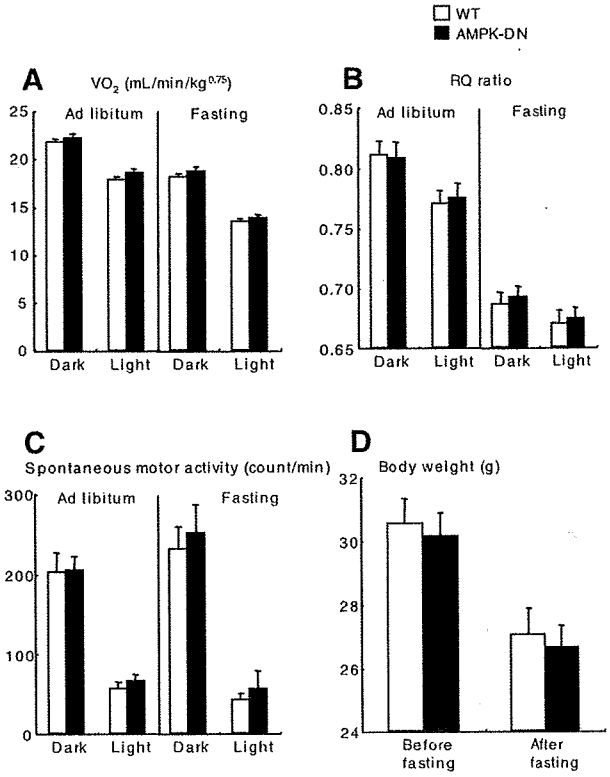

Fig. 2. Oxygen consumption, respiratory quotient (RQ) ratio, and spontaneous motor activity while sedentary and body weight change after 24-h fasting. Oxygen consumption (*A*), RQ ratio (*B*), and spontaneous motor activity (*C*) were measured by open-circuit indirect calorimetry using O_2/CO_2 metabolism measuring system for small animals equipped with an infrared sensor. *D*: body weights were measured before and after fasting. Data are means ± SE of 10 male mice from α_1-AMPK-DN (C line) and 8 male mice from WT (20 wk old). No significant difference is observed between α_1-AMPK-DN vs. WT littermates.

Exercise tolerance of α_1-AMPK-DN mice and WT littermates. First, the ability of α_1-AMPK-DN mice to tolerate an exercise bout was examined. α_1-AMPK-DN (line C) and WT littermates were subjected to two different running intensities on a treadmill. Mice were exercised at a speed of 10 m/min (low intensity) for 30 min and then a speed of 30 m/min (high intensity). Both groups of mice performed well at 10 m/min. However, at a speed of 30 m/min, some α_1-AMPK-DN mice could not continue running for 5 min and most of them dropped out before 30 min (Fig. 3*A*). At a speed of 10 m/min, α_1-AMPK-DN mice and WT mice were able to run for up to 6 h with seven periods of 10 min spent at rest.

To elucidate the mechanism that underlies the intolerance in a high-intensity exercise, muscle glycogen was measured (Fig. 3*B*). The glycogen content in α_1-AMPK-DN mice before exercise was 37% lower than that in WT littermates. Although only mice that were able to tolerate exercise were examined, at 10 min after the high-intensity exercise plus 30 min of low-intensity exercise, glycogen content was reduced by 1.12 and 1.54 μmol/g wet tissue in WT littermates and α_1-AMPK-DN mice, respectively, suggesting that both groups of mice had performed a substantial amount of running.

After the 6-h low-intensity exercise, we measured skeletal muscle AMPK activity in α_1-AMPK-DN (line C) mice and